

Sponsored by the



Saint Petersburg  
State University  
[www.spbu.ru](http://www.spbu.ru)



CONVERGENT SCIENCE AND  
TECHNOLOGY FOR SOCIETY

# PARTICIPANT'S TALKS

21-28 August 2016  
Repino, Russia

[www.raciri.org](http://www.raciri.org)

# **PARTICIPANT'S TALKS**

# CONTENTS

<b>Luis Aguilera</b> .....	1
<b>Valentin Akkuratov</b> .....	2
<b>Olga Alekseeva</b> .....	3
<b>Evgeniy Altynbaev</b> .....	4
<b>Nuraly Amirov</b> .....	5
<b>Daria Andronikova</b> .....	6
<b>Kuralai Ashikkalieva</b> .....	7
<b>Ivan Atknin</b> .....	8
<b>Timo Bisswanger</b> .....	9
<b>Anastasiia Boikova</b> .....	10
<b>Yury Cherepennikov</b> .....	11
<b>Alena Degtiarenko</b> .....	12
<b>Petr Dobrokhotov</b> .....	13
<b>Gleb Dovzhenko</b> .....	14
<b>Ola Kenji Forslund</b> .....	15
<b>Kristina Galdina</b> .....	16
<b>Yaroslav Gevorkov</b> .....	17
<b>Sergey Gizha</b> .....	18
<b>Jakob Gollwitzer</b> .....	19
<b>Svetlana Gorodzha</b> .....	20
<b>Kseniia N. Grafaskaia</b> .....	21

<b>Jan Gruenert</b> .....	22
<b>Ekaterina Iashina</b> .....	23
<b>Kseniia Ilina</b> .....	24
<b>Nikolay Kameko</b> .....	25
<b>Fedor Kashaev</b> .....	26
<b>Julia K. Keppler</b> .....	27
<b>Aleksandr Klyuyev</b> .....	28
<b>Irina Kolesnikova</b> .....	29
<b>Nickolay Kolyshkin</b> .....	30
<b>Artem Korshunov</b> .....	31
<b>Ksenia Kozlovskaya</b> .....	32
<b>Elena Kuchma</b> .....	33
<b>Elena Kuznetsova</b> .....	34
<b>Charlotte Lorenz</b> .....	35
<b>Lisa K. Mahnke</b> .....	36
<b>Nikita Marchenkov</b> .....	37
<b>Margarita Marchenkova</b> .....	38
<b>Leonid Mazaletskiy</b> .....	39
<b>Svetlana Medvedeva</b> .....	40
<b>Masoud Mehrjoo</b> .....	41
<b>Irina Miloichikova</b> .....	42
<b>Tatiana Mishurova</b> .....	43

<b>Alexander Mistonov</b> .....	44
<b>Dmitrii Nesterov</b> .....	45
<b>Evelina Nikelshparg</b> .....	46
<b>Fan Pan</b> .....	47
<b>Elena Parinova</b> .....	48
<b>Ilia Petrov</b> .....	49
<b>Petai Pip</b> .....	50
<b>Mikhail Platunov</b> .....	51
<b>Igor Plokhikh</b> .....	52
<b>Philipp Polzin</b> .....	53
<b>Yuriy Potrakhov</b> .....	54
<b>Elena Povarova</b> .....	55
<b>Alla Pustovalova</b> .....	56
<b>Salim Reza</b> .....	57
<b>Janina Roemer</b> .....	58
<b>Irina Safiulina</b> .....	59
<b>Martin Seyrich</b> .....	60
<b>Ivan Shishkin</b> .....	61
<b>Dmitrii Shuleiko</b> .....	62
<b>Dmitri Smirnov</b> .....	63
<b>Roman Sundeev</b> .....	64
<b>Olesya Timaeva</b> .....	65

<b>Gennadiy Timofeev</b> .....	66
<b>Elena Ushakova</b> .....	67
<b>Gleb Valkovskiy</b> .....	68
<b>Polina Vanina</b> .....	69
<b>Torsten Veltum</b> .....	70
<b>Egor Vezhlev</b> .....	71
<b>Oksana Yurkevich</b> .....	72
<b>Tatiana Zakharchenko</b> .....	73
<b>Peng Zhang</b> .....	74

## **Luis Aguilera**

[aguilera@chalmers.se](mailto:aguilera@chalmers.se)

Chalmers University of Technology

Department of Physics

**PhD candidate**

SE-412 96, Göteborg, Sweden

**Research interests:** lithium ion batteries, mesoscopic structure in liquids, large scale facilities



### **Effects of LiTFSI on the nanostructure of imidazolium and pyrrolidinium based ionic liquids**

In the recent years, ionic liquids (IL) have attracted attention of the research community due to their outstanding properties and the benefits that can be achieved if implemented into Lithium ion Batteries [1]. A number of studies, both experimental (small angle X-ray scattering-SAXS) [2] and simulations (molecular dynamics-MD) [3], have suggest that unlike traditional molecular liquids, ILs are characterized by heterogeneities at a nanoscopic scale.

In this work, we investigate the effect of Lithium salt doping (lithium bis(trifluoromethanesulfonyl)imide) (LiTFSI) on the nanoscale segregation of two kinds of ionic liquids, N-Alkyl-N-methyl-Pyrrolidinium ( $\text{Pyr}_{1n}$ -TFSI) and 1-Alkyl-3-Methylimidazolium ( $\text{C}_n\text{mim}$ -TFSI) ( $n=3, 4, 6$  and  $8$ ) both containing TFSI anions, by means of SAXS and FT-Raman spectroscopy.

Interestingly enough, the nanoscale heterogeneities prevail despite the strong influence of the lithium ions on the anions. However, the middle range ordering, attributed to the TFSI anion, is affected by the Li-salt doping as formerly predicted by Raman measurements.

[1] M. Armand and J. M. Tarascon, 164 (2008).

[2] A. Triolo, O. Russina, B. Fazio, G. B. Appetecchi, M. Carewska, and S. Passerini, *Soft Matter* **130**, 1395 (2009).

[3] B. L. Bhargava, R. Devane, M. L. Klein, and S. Balasubramanian, *Soft Matter* (2007).

## **Valentin Akkuratov**

[akkuratov.val@gmail.com](mailto:akkuratov.val@gmail.com)

Shubnikov Institute of Crystallography of Federal Scientific Research  
Centre "Crystallography and Photonics" of Russian Academy of  
Sciences, Laboratory of X-Ray analysis methods and synchrotron  
radiation

**Engineer**

119333, Russia, Moscow, Leninsky Prospect, 59

**Research interests:** physics of condensed matter, synchrotron  
radiation, X-ray diffraction analysis methods



### **X-ray and neutron diffraction non-mechanical control optics: development & application**

Currently, X-ray and neutron radiation are one of the most effective methods of studying the structure and properties of materials with nanometer and angstrom resolution. [1] This choice is motivated by the fact that they are non-destructive and highly accurate. There are three main options required for using X-ray or neutron radiation as a tool for studying the structure: collimation, monochromatization and control. Usually a large number of X-ray or neutron optical elements is needed for preparation of beam with desired parameters. At the same time, the restructuring of the experimental conditions may cause some difficulties.

The use of mechanical control imposes significant limitations on the ability of quick adjustment of beam parameters. On the other hand, the use of ultrasound for a controlled modulation of the lattice parameter is a simple, and probably the most effective way to non-mechanical control. Recently was shown that long-wave ultrasound can be used to control the spatial and spectral characteristics of the X-ray beam with high precision and time resolution [2].

In terms of creating a regular strain conditions using ultrasonic vibrations in crystals, most promising are bending vibrations in Bragg geometry and longitudinal oscillations along the length of the crystal in the Laue geometry. Such variations allow us to create periodically in time and uniform within footprint of beam vibrations. Therefore, acoustic resonator (operating in bending or longitudinal vibrations mode) is the key element which necessary for the implementation of non-mechanical control of neutron or x-ray beam.

Ultrasonic standing wave in resonator was excited by applying electric field at a resonance frequency (less than 200 kHz). As a result, in the optical part of resonator occur ultrasonic vibrations with wavelength of tens of millimeters which is several times greater than the beam width. With this dynamic control of the lattice parameter it's possible to make several important things: scan the diffraction parameter, change the emission spectrum, control the divergence of the beam, recording rocking curves.

The aim of present work is the description of the technologies and main stages of development and applying of adaptive elements for X-ray and neutron optics.

[1] M.V. Kovalchuk, S.I. Zheludeva, V.L. Nosik, X-rays – from volume to the surface // Nature 1997.№2

[2] A.E. Blagov., M.V. Kovalchuk, V.G. Kohn et al., JETP. 2005. T.128. Vol. 5 (11), 893.

## **Olga Alekseeva**

[blackhole2010@yandex.ru](mailto:blackhole2010@yandex.ru)

Peter the Great St.- Petersburg Polytechnic University

**PhD student**

Russia, 195251, St.Petersburg, Polytechnicheskaya, 29

**Research interests:** Physics of solid state, Ferroelectrics, Nanostructures, Nanocomposites, Low-dimensional systems



### **Dielectric and crystal structure study of the ferroelectric composites (1-x)NaNO<sub>2</sub>+(x)BaTiO<sub>3</sub> and (1-x)KNO<sub>3</sub>+(x)BaTiO<sub>3</sub>.**

The results of complex research of powder mixtures (1-x)NaNO<sub>2</sub>+(x)BaTiO<sub>3</sub> and (1-x)KNO<sub>3</sub>+(x)BaTiO<sub>3</sub> at different concentrations of BaTiO<sub>3</sub> admixture are reported. The study of dielectric properties of composites (1-x)NaNO<sub>2</sub>+(x)BaTiO<sub>3</sub> at x=0.05 and 0.1 [1] has shown that upon heating at low frequencies  $f < 10$  Hz temperature dependencies of dielectric permittivity and dielectric loss tangent have additional maximum at  $T \approx 420$  K besides the maximum at the Curie temperature of pure NaNO<sub>2</sub>  $T_c = 437$  K. Upon cooling the value of this maximum is significantly less than upon heating. The observed anomaly of the composite dielectric response is suggested [1] to relate with phase transition (PT) of NaNO<sub>2</sub> to incommensurate phase (IP) at  $T \approx 420$  K that indicates significant broadening of temperature range where IP of NaNO<sub>2</sub> exists in the composites comparing with pure NaNO<sub>2</sub>, where IP exists in a narrow temperature range 1-1.5 K near  $T_c$ .

Neutron diffraction measurements of the composites and pure NaNO<sub>2</sub> have been performed. Temperature dependencies of ferroelectric order parameter  $\eta(T)$  have been obtained. Any peculiarities of  $\eta(T)$  of the composites comparing with  $\eta(T)$  of pure NaNO<sub>2</sub> have not been revealed near  $T \approx 420$  K. Frequency dependencies of real and imaginary parts of the dielectric permittivity have been analyzed. Low-frequency relaxation processes (characteristic relaxation frequency  $f \sim 0,1-10$  Hz) have been revealed in the composites with the temperature maximum at  $T \approx 420$  K upon heating. In pure NaNO<sub>2</sub> these process with close frequency value have maximum only at  $T_c$ . At about the same temperature  $T \approx 420$  K temperature maximum of DC-conductivity of the composites is observed. The results of structure and dielectric study allow to suppose the relation of dielectric response anomaly in the composites with processes of charge accumulation and resorption at the boundaries of BaTiO<sub>3</sub> particles.

The temperature evolution studies of (1-x)KNO<sub>3</sub>+(x)BaTiO<sub>3</sub> composites structures have revealed the increase of temperature range where KNO<sub>3</sub> ferroelectric phase exists.

[1] E.V. Stukova, et al., St. Petersburg State Polytechnical University Journal. Physics and Mathematics. 22-27 (2012) 330 №4.

**Evgeniy Altynbaev**  
[evgeniy.alt@lns.pnpi.spb.ru](mailto:evgeniy.alt@lns.pnpi.spb.ru)

PNPI

**Researcher**

Orlova Roscha, Gatchina, Leningrad district, 188300, Russia

**Research interests:** small-angle neutron scattering, exotic spin structures, magnetic phase transitions, magnetic dynamics



## **Spin waves in full-polarized state of Dzyaloshinskii-Moriya helimagnets: Small-angle neutron scattering study**

The competition between the ferromagnetic exchange interaction  $J$  and the antisymmetric Dzyaloshinskii-Moriya (DM) interaction  $D$  leads to appearance of the helical magnetic structure in the cubic B20-type compounds. The external magnetic field  $H_{C2}$  is needed to transform the helix with wave vector  $|\mathbf{k}_s| = D/J$  into the ferromagnetic collinear full-polarized (FP) state [1]. Despite of parallel ordering of the spins in the FP state, presence of the DM interaction leads to the chirality of the dispersion relation of the spin waves. The dispersion relation in this case can be written as follows:  $\varepsilon_{\mathbf{q}} = A(\mathbf{q} - \mathbf{k}_s)^2 + H - H_{C2}$ , where  $A$  is the spin-wave stiffness [2]. To verify the main peculiarities of the helimagnon spectrum in the FP state we have applied small angle scattering of polarized neutrons (SANS). MnSi crystal was chosen for this study as one of the best-known representatives of the DM helimagnets. We have shown that the cross section contains a polarization-dependent part due to the asymmetry of the aforementioned dispersion relation. The last means that the scattering on spin-waves in the FP state of helimagnets can be distinguished by the subtraction of the measured intensities with the different polarization of the incident neutrons from each other:  $I^{SW}(\theta) = I(\theta; +P_0) - I(\theta; -P_0)$ . As can be seen, the inelastic scattering of neutrons on magnons appears mostly around the former Bragg peak in the small angles estimated to be less than  $\theta_0 = \hbar/(2m_n A)$ , where  $m_n$  is the mass of the neutron. By analyzing SANS maps, one can extract the value of the spin-wave stiffness of the system. We have shown that the spin-wave stiffness  $A$  for MnSi helimagnet decreased twice as the temperature increases from zero to the critical temperature  $T_C$  [3].

[1] P. Bak, M. H. Jensen, J. Phys. C, **13**, L881 (1980).

[2] M. Kataoka, J. Phys. Soc. Jpn., **56**, 3635 (1987).

[3] S. V. Grigoriev et al., Phys. Rev. B, **92**, 220415(R) (2015).

**Nuraly Amirov**

[nooreek@list.ru](mailto:nooreek@list.ru)

Department of quantum field theory

**Postgraduate**

36 Lenin Ave., Tomsk, Russia 634050

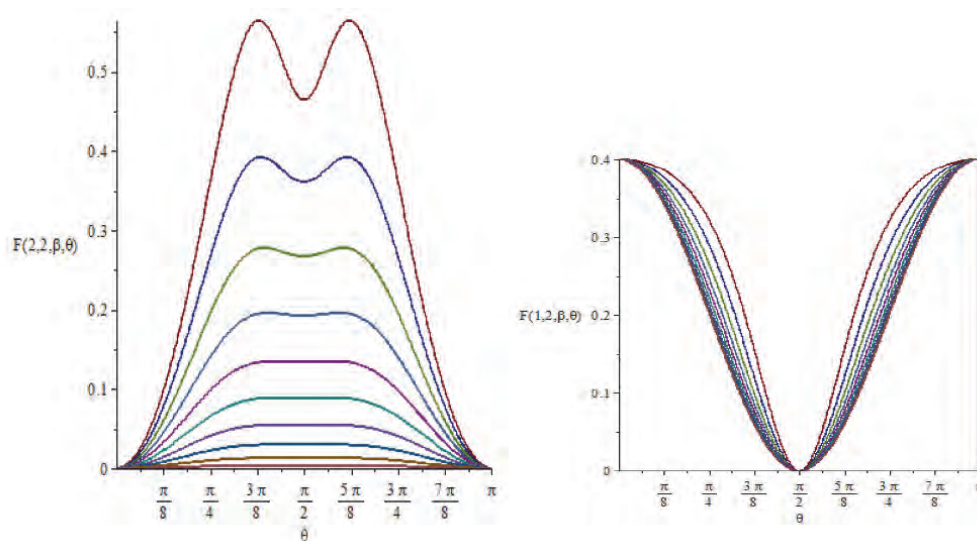
**Research interests:** Synchrotron radiation, Quantum field theory,  
Gravitation and cosmology



## **Polarization of the allocated harmonicas in the case of synchrotron radiation**

The purpose of that research is to define angular maximum of synchrotron radiation. It would help to detect hard photons on the different types of accelerators and colliders in future. Using quantum field theory, Klein–Gordon equation for non-spin particle and Dirac equation for half-spin particle, Laguerre Polynomial we will obtain two components of linear polarization of the radiation of the particle in the low excited state.

The analysis showed a deviation of the angular maximum while the velocity of radiating particle increases. As we can see on the graphics there is no deviation for the particle in the first excited state, but when we go through the deep research the observation of maximum deviation becomes real. Obviously, the higher energy level we paste the more deviations we observe.



Polarization function  $F$  for  $\nu=2$ (left) and  $\nu=1$ (right) for different velocities  
( $\beta=0.1, 0.2, 0.3, 0.4, 0.5, 0.6, 0.7, 0.8, 0.9, 1$ )

In the final analysis we define angular maximum of the power of radiation between  $0.25\pi$  and  $0.36\pi$  first interval and  $0.64\pi$  and  $0.75\pi$  second interval for  $\beta \geq 0.8$ . All calculations carried out in Maple are extremely accurate and allow us to detect hard photons in the most possible angle.

**Daria Andronikova**  
[andronikova.daria@gmail.com](mailto:andronikova.daria@gmail.com)

Ioffe Institute

**PhD student**

26 Politekhnikeskaya, St Petersburg 194021, Russian Federation

**Research interests:** Phase transitions; lattice dynamics; X-ray scattering; ferroelectric material, antiferroelectric materials



## **Phase transitions in lead zirconate titanate single crystals with low Ti content studied by X-ray scattering techniques**

Andronikova D.A.<sup>1,2</sup>, Bronwald I.A.<sup>2</sup>, Burkovsky R.G.<sup>2</sup>, Leontyev I.N.<sup>3</sup>, Leontiev N.G.<sup>4</sup>, Bosak A.A.<sup>5</sup>, Chernyshov D.Y.<sup>6</sup>, Filimonov A.V.<sup>2</sup> and Vakhrushev S.B.<sup>1,2</sup>

<sup>1</sup> Ioffe Institute, Russia, <sup>2</sup> Peter the Great St. Petersburg Polytechnic University, Russia, <sup>3</sup> Southern Federal University, Russia, <sup>4</sup> Azov Black Sea Engineering Institute, Russia, <sup>5</sup> European Synchrotron Radiation Facility, France, <sup>6</sup> Swiss-Norwegian Beamlines at the European Synchrotron Radiation Facility, France

Lead zirconate titanate  $\text{PbZr}_{1-x}\text{Ti}_x\text{O}_3$  (PZT) is one of the most known ferroelectrics. The wide acceptance of PZT can be explained by its high piezoelectric parameters [1]. Interest in PZT is also caused by the variety of properties which it exhibits depending on composition [2, 3, 4].

In the region of high titanium concentrations, only one phase transition to the tetragonal ferroelectric phase [5] is observed. In the region of high zirconium concentrations. At titanium concentrations  $0.05 < x < 0.35$  there are two rhombohedral phases differing by oxygen octahedron rotations [6]. At titanium concentrations  $0 < x < 0.05$  PZT exhibits two phase transitions: the transition from the paraelectric phase with cubic perovskite symmetry to the intermediate phase whose symmetry was determined as rhombohedral [7], and the transition from the intermediate phase to the antiferroelectric orthorhombic phase [8]. It has been reported [9, 10, 11] that the morphotropic phase interface between antiferroelectric orthorhombic and ferroelectric low-temperature rhombohedral phases is observed at  $x = 0.05\text{--}0.06$ .

Although high Zr concentration region of the PZT phase diagram is complex, it is not so well studied. One of the reasons is the lack of the high quality single crystals.

To study the mechanisms of the phase transitions in high Zr PZT we studied PZT single crystals with 0.7 and 1.5% of Ti concentrations by several X-ray scattering techniques. In the presentation the results of X-ray diffraction, diffuse scattering and inelastic X-ray scattering measurements will be presented.

- [1] G. H. Haertling, Journal of the American Ceramic Society 82(4), 797 (1999).
- [2] I. Grinberg, V. R. Cooper, and A. M. Rappe, Nature 419(6910n), 909 (2002).
- [3] F. Cordero, F. Trequatrini, F. Craciun, and C. Galassi, Journal of Physics: Condensed Matter 23(41), 415901, (2011).
- [4] B. Jaffe, W. J. Cook, and J. Jaffe, Piezoelectric Ceramics (Academic Press, London, 1971).
- [5] G. Shirane and S. Hoshino, Physical Review 86, 248 (1952).
- [6] A. M. Glazer, S. A. Mabud, Acta Cryst. B34, 1060 (1978)
- [7] Z.i Xu, X. Dai, D. Viehland, D. A. Payne, Z. Li, Y. Jiang Journal of the American Ceramic Society, 78, 2220, (1995)
- [8] G. Shirane and A. Takeda, Journal of the Physical Society of Japan 7, 5 (1952).
- [9] M. D. Glinchuk, R. O. Kuzian, Journal of the Korean Physical Society, 32, S121 (1998)
- [10] K. Leung, E. Cockayne, and A. Wright, Phys. Rev. B, 65(21), 214111 (2002).
- [11] Ghosh A., Damjanovic D., Applied Physics Letters, 99,23 (2011)

## **Kuralai Ashikkalieva**

[kuralay.physics@mail.ru](mailto:kuralay.physics@mail.ru)

National Research Nuclear University MEPhI

**PhD student**

Kashirskoe Shosse 31, 115409, Moscow, Russia.

**Research interests:** Laser microstructuring of diamond bulk



### **Internal structure of laser-induced conductive wires in diamond bulk**

Laser processing is successfully used for fabrication of buried conductive wires in diamond bulk based on phase transition of diamond to graphenic carbon ( $sp^2$  phase) under laser irradiation [1]. By translating the laser focal plane through the diamond crystal it is possible to fabricate extended conductive wires in diamond. To create the wires with controlled properties the detailed investigations of internal structure of laser-modified diamond are needed. Here we report for the first time on the peculiarities of internal structure of the laser-induced wires in diamond bulk.

In this study, a set of inclined conductive wires was fabricated inside CVD single crystal diamond at different values of scanning velocity and laser pulse energy by Ti:sapphire-laser irradiation ( $\lambda=800\text{nm}$ ,  $f=1\text{KHz}$ ,  $\tau=5\text{ps}$ ). The buried wires were exposed to the surface by mechanical polishing; the obtained cross-sections were carefully examined by means of scanning electron microscopy (SEM) and Scanning Spreading Resistance Microscopy (SSRM). In addition, to characterize the electrical resistivity of laser-induced wires, the I-V measurements were carried out using an automatic system for electrophysical characterization (ASEC-3).

We have found out that only small part of diamond transforms to the  $sp^2$  phase in the region of laser processing. The  $sp^2$  phase is localized within cracks forming a conductive net of nanosheets, while the gaps between the cracks are filled by diamond. The conductive net of nanosheets is spatially arranged in the form of quasi periodic segments having several microns of the size. Each of the segments contains two inclined “basic” cracks, the space between which is filled by parallel periodic nanosheets ( $\sim 150\text{nm}$  in width) inclined to an axis of a wire practically perpendicularly and separated from each other by diamond gaps. It has been found out that the width of the nanosheets is growing with increasing of scanning velocity, while it is independent of pulse energy. We found correlation between the number of segments per unit length and the integral conductivity of the wires.

[1] T.V. Kononenko, et al., *Diamond & Related Materials*. 264-268 (2011) 20.

## Ivan Atknin

[atknin.ii@physics.msu.ru](mailto:atknin.ii@physics.msu.ru)

Federal Scientific Research Centre «Crystallography and Photonics» of  
Russian Academy of Sciences.

### Researcher

Russia, 119333, Moscow, Leninskii Prospect, 59.

**Research interests:** X-ray diffraction, defect structure, crystal diagnostics, x-ray diffraction under external influence, piezoelectric properties of crystals.



## Development of the complex methods for numerical calculations of double- and multi-crystal rocking curves

The results of experimental and theoretical analysis of the integral rocking curves in the nondispersive X-ray double-crystal diffractometer schemes are discussed. It is shown that under certain conditions the secondary peak, which relates to the  $MoK_{\alpha 2}$ -line of the incident X-ray characteristic radiation, takes place at the non-dispersive rocking curves (Fig. 1). The trapezium and Monte-Carlo numerical methods are used for evaluations of the theoretical double-crystal rocking curves.

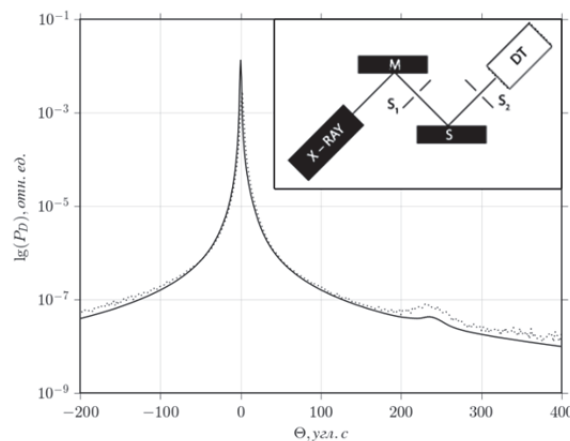


Fig. 1. Theoretical (solid) and experimental (dotted) non-dispersional rocking curves  $P_{2D}(\vartheta)$ : crystal-monochromator and sample are monocrystal Si, diffraction vector  $\mathbf{h} = \langle 220 \rangle$ , Bragg's angle  $\theta_B = 10.64^\circ$ .

The computer program package is elaborated for the numerical calculations of the double- and multi-crystal rocking curves as the mathematical software for the X-ray diagnostics of real crystal structures by the double- and multi-crystal diffractometry methods.

- [1] M.A. Chuev *et al.*, Crystallography Reports. 734-747 (2008) **53**.
- [2] N.V. Marchenkov, F.N. Chukhovskii & A.E. Blagov, Crystallography Reports. 172-176 (2015) **60**.
- [3] P.V. Petrashen, Metallofizika. 35-43 (1986) **8**.
- [4] P.V. Petrashen, F.N. Chukhovskii, Metallofizika. 45-51 (1986) **8**.

## **Timo Bisswanger**

[timo.bisswanger@fu-berlin.de](mailto:timo.bisswanger@fu-berlin.de)

Workgroup of Prof. Reich, Department of Physics

**Master Student**

Free University of Berlin,

Department of Physics, Arnimallee 14, 14195 Berlin, Germany

**Research interests:** (N)EXAFS, XMDC, Raman



### **Resonant Raman investigation of suspended graphene layers on top of locally coupled plasmonic gold structures**

Plasmonic enhancement in Raman scattering is well known as SERS (surface enhanced Raman scattering) and widely used but not fully understood yet [1]. Plasmons can greatly enhance inelastically scattered light like in the Raman process. In the current experiments the plasmonic near-field itself is locally intensified by coupling the surface plasmons to very local hotspot within a nanoscale cavity of gold dimers [2].

Graphene and graphene based  $sp^2$  carbon allotropes like carbon nanotubes or ribbons are well suited for the investigation of this process since the absence of a band gap leads to an unfailling resonance over the visible and ultra violet range [3].

In the preceding works enhancement profiles of symmetric and asymmetric gold profiles on single layer graphene have been investigated [2,4] as well as of single walled carbon nanotubes [5]. To distinguish the scattering process enhanced by the local near-field from the unaffected surrounding area the effect of strain within the cavity is used [4]. The enhancement is very local and spatially below the wavelength of the exciting light though it allows a precise localization of the cavity. The resonance profiles show different enhancement factors actually up to  $10^3$  for incoming and outgoing resonances arising from quantum interference [6].

The current research focuses on varied  $sp^2$  carbon structures, their combinations, and other features coupled in this process.

[1] S. Heeg, PhD thesis, Freie Universität, Berlin, 2015

[2] S. Heeg, et al., Nano Lett. 301-308 (2013) 13(1)

[3] A.C. Ferrari and D.M. Basko, Nature Nanotech 235-246 (2013) 8(4)

[4] S. Heeg, et al., Phys. Stat. Sol. RRL 1067-1070 (2013) 7(12)

[5] S. Heeg, et al., Nano Lett. 1762-1768 (2014) 14(4)

[6] P. Kusch, et al., ArXiv e-prints (2015)

## **Anastasiia Boikova**

[boykova.irk@yandex.ru](mailto:boykova.irk@yandex.ru)

FSRC “Crystallography and Photonics” RAS

**Junior Research Fellow**

119333, Moscow, Leninskii pr., 59

National Research Centre “Kurchatov Institute”

**Research Engineer**

123182, Moscow, Akademika Kurchatova pl., 1

**Research interests:** Protein crystallization, X-ray diffractometry,  
hybrid nanosystems



### **In Situ investigation technique of protein ordered structures formation**

Hybrid organic-inorganic nanosystems including proteins as a functional elements can be basis for new molecular electronic devices [1]. To examine the possibility of using proteins in hybrid structures, it is necessary to prepare crystalline protein films and single crystals, study their properties, and find methods for storing such films and crystals over a long period of time. For this purpose, the special hermetically closed crystallization cell was designed [2]. The cell allows preserving protein crystals in their native state. It consists of the following two main parts: the body and the cup fixed at the base. The materials used for making this crystallization cell and its construction provide the chemical purity of the inner volume of the cell and its impermeability for approximately 4 weeks. The upper part of the inner volume is made up of a light transparent and weakly X-ray absorbing material. This crystallization cell is suitable for optical and X-ray diffraction studies in a wide incident angle range, which enables researchers to perform in situ studies of the nucleation, growth, and degradation of protein crystals.

We investigated the protein lysozyme (hen egg-white lysozyme). Measurements for lysozyme crystals were carried out in different stages of the crystallization process, including crystal nucleation and growth, developed crystals, the degradation of the crystal structure, and complete destruction, using in situ high-resolution X-ray diffractometry.

[1] I Ron, et al., *Acc Chem Res*, 2010, Vol. 43.No 7, pp 945-53.

[2] M. V. Kovalchuk, et al., *Crystallography Reports*, 2014, Vol. 59, No. 5, pp. 679–684.

## Yury Cherepennikov

[che@scalpnet.ru](mailto:che@scalpnet.ru)

National Research Tomsk Polytechnic University

**Master student**

634050, Tomsk, Lenin Avenue, 30

**Research interests:** X-ray physics, Non-Destructive Testing,  
Accelerator physics



### Using acoustic “pumping effect” to produce high-intensive monochromatic X-ray beams

Monochromatic X-ray beams are widely used in modern science for a number of tasks such as X-ray absorption spectroscopy, X-ray structural and elemental analyzes etc. For many kinds of investigation the intensity of the X-ray monochromatic beam is crucial. Nowadays, crystal monochromators are used to produce such beams due to X-ray diffraction. To increase the intensity of monochromatic X-rays beams, the crystals under external influences like electromagnetic field or temperature gradient can be used. Authors of the works [1, 2] observed an increasing of diffracted X-rays from quartz monochromators excited by acoustic wave (“pumping effect”). This effect appears when a frequency of the excited acoustic wave is coincide with the resonant frequency

$$f_n = v/2l,$$

where  $l$  is crystal thickness,  $v$  is sound velocity.

“Pumping effect” allows adjust an intensity of X-ray spectral lines changing an amplitude or frequency of the acoustic field.

In this report experimental results of investigations of spectral characteristics of diffracted X-rays from quartz monochromators are presented. In the experiment quartz crystals with different thickness (0.3, 0.65 and 0.9 mm) we used. Acoustic wave field was initiated in crystals by variable electric field with amplitude from 0 to 50 V and resonant frequencies 9.33, 4.41 and 3.18 MHz, correspondingly.

X-ray tube with the following parameters was used as radiation source:

Voltage – 48 kV;

Current – 1 mA.

The detector BDER-KI-11 was placed in Laue geometry at angles  $5.5^\circ$  and  $4.4^\circ$ . Spectral lines with energies 19.3 and 24.3 keV from all crystal monochromators with and without acoustic excitation were registered. For our conditions the enhancement of output intensity of spectral line under acoustic wave (“pumping effect”) is achieved 5 times at least.

This work was particularly supported by the grant of the Ministry of Education and Science of the Russian Federation within Program "Nauka" number 3761.

[1] R. G. Gabrielyan et al Phys. Stat. Sol. 361-368 (1985) 92

[2] A S Gogolev et al J. Phys.: Conf. Ser. Article number 012019 (2010) 236

**Alena Degtiarenko**

[Alevakhova@gmail.com](mailto:Alevakhova@gmail.com)

NRC “Kurchatov Institute”

**Research engineer/PhD Student**

1, Akademika Kurchatova pl., Moscow, 123182, Russia

**Research interests:** High-temperature superconductors, X-ray diffraction, scanning electron microscopy, electron backscattering diffraction, thin films



## **The characteristics of biaxially textured Cu-based tapes as substrate prototype for 2G HTS**

A.Yu.Degtiarenko, A.S.Ivanov S, S.V.Shavkin, A.V.Ovcharov, P.N.Degtyarenko, E.A.Golovkova

It is well known that biaxially textured substrates based on the Ni-W-alloys are widely used for the manufacturing of second generation high-temperature superconductors (2G HTS). However there are few copper based alloys, which can be a better alternative to the traditional Ni-W alloys due to their low magnetic properties and cost. Cu-based alloys with 1.2 and 1.6 at.%-Fe seem to be the best candidates for this purpose. Initial samples were obtained by the Mikheev Institute of Metal Physics [1]. The samples underwent several investigative techniques in order to estimate their structural parameters, as well as their electrical and magnetic properties in depth.

For the determination of the crystal lattice parameters the X-ray diffraction was used. The microstructure of the samples was investigated by a transmission electron microscope (TEM) Titan 80-300 at accelerating voltage of 300 keV. The cross sections of both types of samples for the TEM were obtained by a focused ion beam (FIB) on the scanning electron microscope Helios FEI. The surface roughness was measured by an atomic force microscope (AFM). The texture features were observed using the electron backscatter diffraction method (EBSD). The resistivity was measured by a standard four probe method in the temperature range from 4.2 up to 300K. Magnetization data were collected by a vibrating sample magnetometer (PPMS Quantum Design) at 5K and at 77K in by a scheme with the perpendicular magnetic to the sample surface.

Based on the data collected during investigations it was established that the lattice parameters  $a$  of the Cu-1.2at.% Fe and Cu-1,6at.% Fe are  $a = 3.6147 \text{ \AA}$  and  $a = 3.6149 \text{ \AA}$ , respectively. This is equal to the lattice parameters of the buffered coatings for 2G HTS. Measured roughness of the surface was  $R_a = 17.84 \text{ nm}$  for Cu-1.2at% Fe and  $R_a = 74.32 \text{ nm}$  for Cu-1.6at% Fe. Analysis of the microstructure showed an overall uniform distribution of iron particles in the entire copper matrix. The typical sizes of the Fe - particles vary from 40 to 50 nm. The fraction of cubic orientation of the alloys was 98% for Cu1,2% Fe and 97% for Cu1,6% Fe, respectively. Magnetization values for Cu1.2%Fe and Cu1.6%Fe were  $M_s < 0.43$  and  $M_s < 1.05 \mu\text{Wb}\cdot\text{m}\cdot\text{kg}^{-1}$  at  $T=5\text{K}$  and  $M_s < 0.15$  and  $M_s < 0.75 \mu\text{Wb}\cdot\text{m}\cdot\text{kg}^{-1}$  at  $T=77\text{K}$ , respectively. The curve for the electrical resistance versus temperature is decreasing up to its minimum at 40K and then increases up to 4.2 K.

The observed results indicate that the biaxially textured copper-based alloys with their excellent price-performance ratio are good substitutes for the Ni-W alloys and can therefore be tested on the Bruker pilot line of the NRC “Kurchatov Institute”.

[1] Yu.V.Khlebnikova, I.V.Gervasyeva, T.R. Suaridze, D.P. Rodionov, L.Yu. Egorova, J. Techn. Phys. Letters 40,19 (2014)

## **Petr Dobrokhotov**

[PLDobrokhotov@mephi.ru](mailto:PLDobrokhotov@mephi.ru)

National Research Nuclear University MEPhI (Moscow Engineering  
Physics Institute)

**PhD Student**

Moscow, Kashirskoe sh., 31

**Research interests:** X-ray texture techniques, Texture and structure  
inhomogeneity, Nuclear materials, ODS steel



### **The use of Generalized Pole Figures method for texture and substructure inhomogeneity evaluation in ferritic-martensitic steels**

Fast-neutron nuclear reactors development imposes high demands on the structural materials: long-term operation of nuclear plant requires of core material high heat resistance, stability under irradiation, low corrosion rate etc. There are several candidate materials for use in the core, among which is Oxide dispersion strengthened (ODS) ferritic-martensitic steels. Addition of oxide particles (mostly  $Y_2O_3$ ) was intended to improve high-temperature strength of ferritic-martensitic steel products, making ODS steels the most promising core material.

Exploitation properties of products are determined by structural condition of material, set during the manufacturing process. In order to obtain the properties needed it is necessary to comprehend structural features imposed by applied treatment. Common methods of research and analysis cannot provide statistically reliable results of materials' structural condition. This study demonstrate the advantages of using original technique of generalized pole figures (GPF) [1] on the ODS steels research.

The GPF method, realizable by texture diffractometers of last generations, includes successive registration of profiles for the same X-ray line at each point of a texture pole figure in the course of its measurement. A profile of X-ray line ( $hkl$ ) characterizes the condition of crystalline lattice along the normal to reflecting planes  $\{hkl\}$ . Thus, the GPF method gives complete information on substructure conditions of grains with different crystallographic orientations and provides insights into possible deformation mechanisms and strain hardening features.

By the means of GPF method it was shown, that deformation imposed during rolling process of tubes made of ODS steel EP450 inhomogeneous through the thickness of the tube. Texture formation in the bulk of the tube wall is suppressed, accompanied with low hardening rate, while external surfaces of tube's wall are characterized by strong texture maxima and high strain hardening rate. Herewith one can distinguish inward and outward surfaces of the tube wall: while inward surface have stronger texture and low deformation level, outward surface is characterized by weaker texture and high deformation level. Through-thickness structural inhomogeneity implies non-uniform properties distribution, which could lead to development of high stress during exploitation of the cladding tube.

[1] Perlovich Yu., Isaenkova M., Fesenko V. *Zietschrift fur Kristallographie*, suppl.26 (2007), pp. 327-332.

## **Gleb Dovzhenko**

[gleb.dovzhenko@hzg.de](mailto:gleb.dovzhenko@hzg.de)

Helmholtz-Zentrum Geesthacht

### **PhD Student**

21502 Geesthacht, Max-Planck-Straße 1.

Material science,

**Research interests:** neutron / synchrotron stress-diffractometry,  
lightweight metal alloys.



## **Residual Stress & Fatigue properties of Ti-6Al-4V Friction Surfacing Coated Sheets**

By the process of Friction Surfacing (FS), coatings are generated from metallic materials at temperatures below their melting range. The applicability of the process has been described for a large number of materials. The process allows for deposition in similar and dissimilar configurations, i.e. layer and substrate materials can be same or not. Layers deposited by FS can extend the service life of components such as turbine blades, rails and medical implants by repairing worn parts, reducing wear and improving anticorrosion properties, increasing stiffness. Such an additive approach avoids the requirement to machine components with initially larger cross sections, and it can be applied in a flexible manner. Since no melting of the coating or the substrate material occurs, dilution can be completely avoided. For light-weight materials in the transportation sector, e.g. aerospace, alloys like Ti-6Al-4V or high strength aluminium alloys are candidates for such treatment.

FS involves thermal and mechanical processing of coating and substrate, which leads to changes in residual stress state for both of them. Different FS parameters result in different thermal cycles and different coating strip geometries. The first goal of current investigation is to determine the correlation between residual stress state of coated thin Ti-6Al-4V sheets and FS parameters, namely translational speed. Second goal is to determine how that state affects mechanical properties, namely wear.

Preliminary results show that stress state of sheets after FS treatment is very similar to the state of butt-welded sheets. Tensile residual stresses in coating grow higher with rise of translational speed (meaning higher temperature gradients). As for mechanical properties, for a chosen crack propagation direction to be orthogonal to coating strip, coated samples can withstand 100 times more load cycles compared to base material.

## Ola Kenji Forslund

okfo@kth.se

Department of Materials & Nano Physics,  
KTH Royal Institute of Technology, Kista, Sweden

**PhD Student** – Energy Materials

Electrum 229, SE-16440 Kista, Sweden

**Research interests:** Energy materials, neutron scattering, muon spin rotation



### Neutrons & Muons for the Next Generation Energy Materials

To accomplish a paradigm shift in the field of energy related materials and future solid state energy devices, it is central to understand the fundamental dynamical processes that govern the transfer of energy on an atomic scale. Here new possibilities have opened through recent developments in state-of-the-art neutron/muon spallation-sources and forthcoming free electron lasers. While Li-ion batteries are considered the main candidate for mobile energy storage applications, compounds based on lithium's heavier cousin, sodium (Na) have recently started to receive a lot of attention. One reason is that our Li-reserves are limited and to realize future electric vehicles we might have to reconsider the Li-ion technology. Na has indeed many advantages over Li e.g. Na is one of the most abundant elements in nature (earth's crust as well as in normal seawater of our great oceans), which makes it about 5 times cheaper than Li. Further, Na-ion batteries are also much less toxic and easier to recycle. My recently started PhD project has two main focus points:

1. To in detail understand how subtle structural changes control ionic diffusion on an atomic scale. I will focus on comparative studies of established Li-/Na-ion battery compounds in order to obtain a consistent understanding. In addition, I intend to open the characterization of a several new promising battery cathode materials. The experimental data will also be combined with *ab initio* computational models.
2. Recent work on Na-ion batteries revealed that a substantial enhancement in diffusion rate can be achieved by rather moderate microscopic pressures in e.g. strained thin films and possibly also nano-particles. The aim is to assess if such effect is a general behaviour among intercalated ionic materials and to understand the underlying mechanism.

For this project I intend to use large-scale experimental facilities and techniques including neutron diffraction (atomic and magnetic structure) [1], inelastic neutron scattering (phonons and ion diffusion) [2] as well as muon spin rotation/relaxation (magnetic order and ion diffusion) [3]. The project is a collaboration between KTH, Toyota Central R&D Labs., Paul Scherrer Institute (PSI), ETH Zurich and ISIS pulsed neutron/muon source.

This research is financed by the Swedish Research Council (VR).

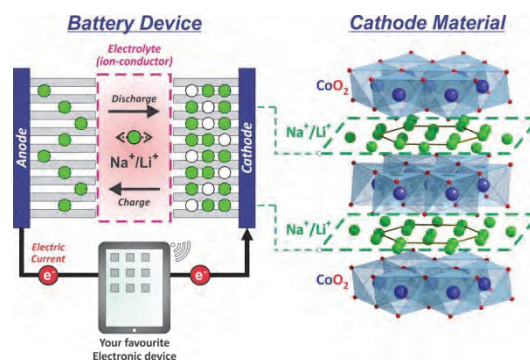


Fig.1: Schematic view of a battery device and cathode material on the atomic scale.

[1] M. Medarde, M. Månsson *et al.*, Phys. Rev. Lett. **110**, 266401 (2013)

[2] Juranyi, Månsson *et al.*, EPJ Web of Conf. 83, 02008 (2015)

[3] J. Sugiyama, M. Månsson *et al.*, Phys. Rev. Lett. **103**, 147601 (2009)

## **Kristina Galdina**

[kris-galdina@mail.ru](mailto:kris-galdina@mail.ru)

Saint Petersburg State University,

**Master student**

Ulianovskaya Street, 3, Petrodvorets, St. Petersburg, 198504, Russia

**Research interests:** Lithium-ion batteries, X-ray spectroscopy,  
synchrotron radiation



### **High capacity Li-rich cathode materials for Li-ion batteries: study of the structure changing during charge and discharge processes.**

Lithium-ion batteries (LIBs) are promising power supplies for use in electric vehicles due to their high energy density and long cycling life relative to other secondary batteries. Traditionally,  $\text{LiCoO}_2$  is used as a cathode material for LIBs. But using this structure leads to several drawbacks such as a poor structural stability, an extract all lithium ions and toxicity of cobalt. Therefore, it is important to develop alternative cathode materials in order to obtain a higher capacity, improved safety and lower cost [1]. It has been shown [2] that transition metal mixed oxide can satisfy these requirements.

One of the promising cathode materials for LIBs is  $\text{LiNi}_{0.8}\text{Mn}_{0.1}\text{Co}_{0.1}\text{O}_2$  structure. This structure combines benefits for  $\text{LiCoO}_2$  and  $\text{LiNiO}_2$  such as structural cycling stability, higher capacity, improved safety and lower cost [3]. The presence of Mn in the structure provides the cycling performance. Nevertheless, the detailed evolution of the local structure around the ions of nickel, manganese and cobalt during one charge / discharge cycle is unclear up to now. In this connection the current work is directed to careful study of changes of local structure around the metal (Me) ions in the  $\text{LiNi}_{0.8}\text{Mn}_{0.1}\text{Co}_{0.1}\text{O}_2$  structure during one charge / discharge cycle.

According to [4], the oxidation state of manganese is not changed during the charge and discharge processes. In contrast to this result analysis of Mn  $L_{2,3}$ -absorption spectra carried in the current work reveals that during the process of discharging the oxidation state of manganese is varied from  $\text{Mn}^{4+}$  to  $\text{Mn}^{3+}$  and back to  $\text{Mn}^{4+}$  for a completely discharged sample. Moreover, the similar situation was traced for cobalt, which also changes the oxidation state in the process of discharge from  $\text{Co}^{3+}$  to  $\text{Co}^{2+}$  and back to  $\text{Co}^{3+}$  for the full discharged sample. The greatest changes were found for nickel ions. It was established that pristine structure  $\text{LiNi}_{0.8}\text{Mn}_{0.1}\text{Co}_{0.1}\text{O}_2$  is characterized by a mixed oxidation states  $\text{Ni}^{2+}/\text{Ni}^{3+}$ . During the charge process the oxidation state  $\text{Ni}^{3+}$  becomes dominant. But discharge process leads to the formation of the predominantly  $\text{Ni}^{2+}$  oxidation state.

Nevertheless, in the completely discharged sample the oxidation state of nickel coincides with the original structure. One can conclude that the presence of nickel in the structure provides a cycling stability of structure.

All the studies were carried out by near edge x-ray absorption fine structure (NEXAFS) spectroscopy method. The NEXAFS measurements were performed at the RGL-station on the Russian-German beamline at the BESSY II synchrotron light source of the Helmholtz-Zentrum Berlin.

[1] D. L. Vu, et al., Korean J. Chem. Eng. 514-526 (2016) 33

[2] M. S. Whittingham, Chem. Rev. 4271-4301 (2004) 104

[3] P. Kalyani, et al., Sci. Technol. Adv. Mater. 689-703 (2005) 6

[4] B. J. Hwang, et al., Chem. Mater. 3676-3682 (2003) 15.

**Yaroslav Gevorkov**  
[yaroslav.gevorkov@desy.de](mailto:yaroslav.gevorkov@desy.de)

DESY

**PhD Student**

Notkestraße 85, 22607 Hamburg

**Research interests:** Real-time data processing, Pattern recognition,  
Algorithms for X-ray crystallography



## **Real-time data processing for serial crystallography experiments**

Serial crystallography allows structure determination of biological macromolecules from small crystals that are not useable for conventional analysis. Crystals in random orientation are placed into the beam of a pulsed X-ray source to acquire one single diffraction pattern from one crystal. The X-ray sources typically are X-ray Free Electron Lasers (XFELs) that can deliver a very high radiation dose, far in excess of what the crystal could normally tolerate, in a time span in the range of femtoseconds. The crystal diffracts the X-rays before it is destructed (diffraction before destruction principle), overcoming the effect of radiation damage [1].

The collected diffraction patterns are indexed individually and merged together to obtain the volume of structure factors. For a good reconstruction, a large number of diffraction images is needed (typically tens of thousands patterns). Due to the limited availability of beam time, the optimization of the collection process is crucial for obtaining good results. Therefore, the real-time analysis and monitoring of the collected data is of great interest. We develop algorithms and tools that are capable of meeting real-time constraints of current X-ray sources (Typically 20 – 120 Hz) while retaining or improving the results compared to the conventional methods of choice. The algorithms are collected in the OnDA software suite.

This poster shows two recently developed and implemented algorithms that were able to significantly speed up the processing pipeline. The first is called “streakFinder”, it masks artefacts in the diffraction image that are caused by the liquid jet sample delivery system. The second is called “peakFinder9”, it fulfills the well-known task of peak finding in diffraction images. Having a set of filter rules that filter out peak candidates in an early stage, this peak finding algorithm allows to have an accurate and costly background estimation while still being real-time capable.

[1] Chapman et al. J. "Femtosecond diffractive imaging with a soft-X-ray free-electron laser". Nature Physics 2006, 2 (12), 839-843.

## Sergey Gizha

[Sgizha@gmail.com](mailto:Sgizha@gmail.com)

P.N. Lebedev Physical Institute of the RAS

Scientific employee

53 Leninskiy Prospekt, 119991, Moscow, Russia

**Research interests:** X-ray spectrometry, X-ray reflectometry, X-ray diffraction



### The Notch Spectral Filter for Energy-Dispersive X-ray Spectrometry

S. Gizha, A. Touryanski, I. Pirshin, V. Senkov

The possibility of an effective band reject filtration of a continuous X-ray excitation spectrum in an energy range  $E \geq 8$  keV is shown. This enables a drastic increase in sensitivity of energy dispersive X-ray spectrometry in detection of weak fluorescent lines. Optimum conditions for the rejection of the given spectral band with an intensity attenuation of  $>20$  dB are achieved with the use of a spaced row of thin film monochromators made of high oriented pyrolytic graphite (HOPG)[1]. Statistical fluctuations of the elastically scattered radiation background are reduced by combining the bottom of a created spectral valley and with the position of an analyzed fluorescence line. The proposed band reject filtering scheme allows also effective suppressing of intense characteristic lines in the primary and scattered radiation spectra.

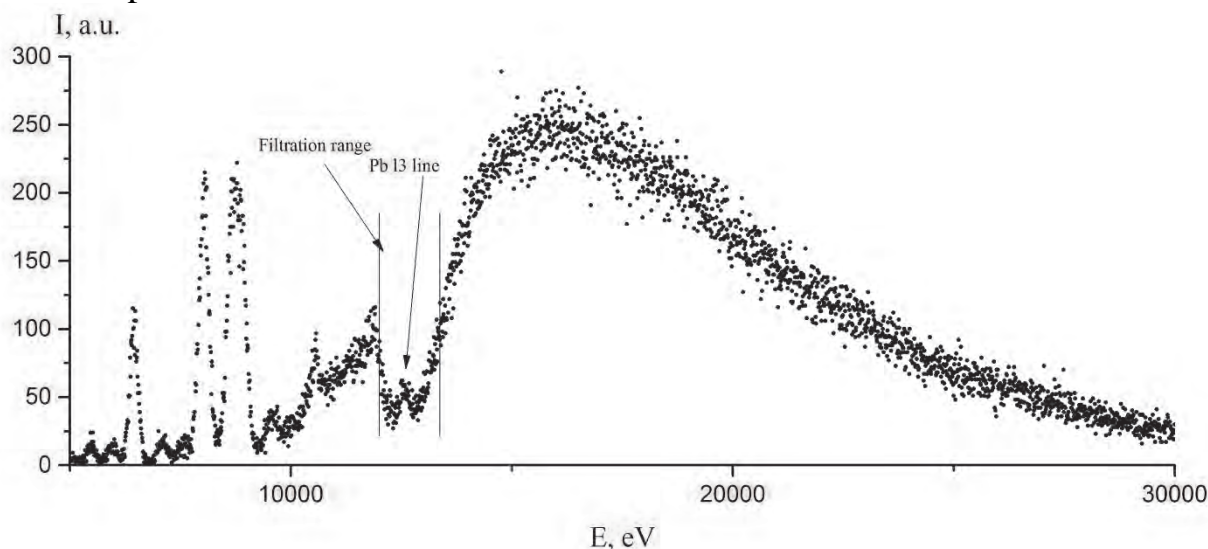


Fig.1. Experimental results.

On fig.1 experimental results are shown. The experiment was performed on CompleXRay C6 multifunctional X-ray reflectometer. Initial beam was produced by X-ray tube with copper anode. Polystyrol with small additive of Pb dust was used as a target. HOPG sample with thickness 0.7mm and mosaic angle  $0.95^\circ$  was used to cut off energy range around Pb  $L_\beta$  line, that is 12.6 keV. This allowed effectively decrease statistical noise up to 12 db around that line and made it clearly observable.

[1] Nesterets, Ya I., et al. "Application of the statistical dynamical theory of X-ray diffraction to calculation of the HOPG echelon-monochromator parameters." PHYSICA STATUS SOLIDI A APPLIED RESEARCH 179.2 (2000): 311-318.

## **Jakob Gollwitzer**

[jakob.gollwitzer@desy.de](mailto:jakob.gollwitzer@desy.de)

University of Hamburg

**PhD Student**

Jungiusstr. 11, 20355 Hamburg

**Research interests:** Magnetization Dynamics, X-ray Physics



### **Resolving Standing Spin Waves with Nuclear Resonant Scattering**

In the field of magnonics, the magnetization dynamics of magnetic sample systems are a crucial feature which have been exploited to facilitate a range of technical applications including frequency filters, spin-wave multiplexers[1], and spin wave assisted magnetization reversal[2]. Magnetization Dynamics are usually investigated with inelastic scattering methods such as Brillouin Light Scattering, Raman Spectroscopy, and inelastic neutron scattering. Recently, Nuclear Resonant Scattering (NRS) has been established as an experimental technique sensitive to the magnetization trajectory in permalloy (Ni<sub>80</sub>Fe<sub>20</sub>) thin films excited at ferromagnetic resonance [3]. NRS is a coherent, elastic scattering method which maps the magnitude, orientation, and distribution of the hyperfine field present at <sup>57</sup>Fe nuclei via the Mössbauer resonance of <sup>57</sup>Fe. Use of a <sup>57</sup>Fe Probe layer affords the method a very high depth resolution in magnetic film samples [4].

We employ NRS to investigate the spin dynamics of an array of 800 nm wide permalloy stripes. NRS, in conjunction with micromagnetic simulations, resolves the position dependent spin trajectory in the stripe array excited at ferromagnetic resonance. The presence of standing spin waves in the permalloy stripes is confirmed. The ability of NRS to determine the presence of standing spin waves showcases the method as useful for characterizing the highly position dependent spin dynamics of nano-structured magnetic thin film systems.

In addition, we aim to use NRS to measure dynamically induced magnetic superstructures in nanostructured multilayers. The Bragg peaks associated with such dynamic superstructures are suitable for use in essentially noise free detection of quasiparticle excitations such as phonons and magnons. Such noise free measurements schemes are potentially useful for pump probe experiments studying quasiparticles at FELs.

[1] K. Vogt et al. Nature Communications 4727 (2014)

[2] T. Seki et al. Nature Communications 2737 (2013)

[3] L. Bocklage et al. Physical Review Letters 114, 147601 (2015)

[4] R. Röhlsberger et al. Physical review letters 89, 237201 (2002)

## **Svetlana Gorodzha**

[sveta\\_gorodzha@mail.ru](mailto:sveta_gorodzha@mail.ru)

National Research Tomsk Polytechnic University

**PhD student**

634050, Tomsk, Lenin Avenue, 30, Russia

**Research interests:** 3-D imaging, computed tomography, x-ray imaging, biomaterials, scaffolds, 3-D matrices, polymers, hydroxyapatite



### **Synchrotron micro-computed tomography as a methodology for polymer 3-D scaffolds characterization**

The appearance of synchrotron radiation sources and their optimization for numerous scientific aims paved the way for completely new and significantly improved methods of X-ray analysis for applications in various scientific fields including materials science. Synchrotron radiation allows for the in depth study of the structural properties of matter due to its high quality brightness, brilliance and intensity. That is why synchrotron visualization is widely used technique for the characterization of materials for biomedical application. A tissue engineering material (scaffold) should possess the appropriate mechanical, structural, chemical, and surface properties. Thus, a thorough characterization of the scaffolds is crucial in order to assess their suitability and to understand the biomechanical environment the cells will sense upon seeding. Internal structure of scaffold, pore size and pore distribution, is an important point for its efficiency as biomedical material, as it determines the cellular penetration, extracellular matrix production, and neovascularization of the inner areas of the scaffold [1]. This work is devoted to the properties study of weakly absorbing 3-D polymer matrices with different fiber structure (randomly-oriented and well-aligned) enriched with silicate-containing particles. For investigation of weakly absorbing materials, such as polymers, typically, scanning electron microscopy [2], atomic force microscopy [3], transmission electron microscopy [4] and other methods are used [5]. These standard techniques provide information only in 2-space without accessing in-depth information and do not allow penetrating within material without destroying a sample. For this study we applied micro-computed tomography setup at TopoTomo beamline station of the Synchrotron Light Source ANKA (Karlsruhe, Germany). X-ray absorption tomography is an established method for 3-D imaging. Use of monochromatic, parallel beam available with synchrotron facilities combined with high resolution x-ray detector provided an unique information on 3-D architecture of biomaterials.

Therefore, here we present results, which characterize an internal scaffolds structure such as: pores/particles spatial distribution, fibers directionality, fibers size, and density of the scaffold in a whole volume of the samples.

This research was supported by the Federal Target Program #14.587.21.0013 (a unique application number 2015-14-588-0002-5599, project in the frames of ERA.NET RUS Plus – S&T Call, #58 INTELBIOCOMP) and MK-6459.2016.8.

[1] C. Renghini, et al., *J. Eur. Ceram. Soc.* 1553-1565 (2013) 13

[2] L. Mousnier, et al., *Int. J. Pharm.* 10-17 (2014) 471

[3] E. Balnois, et al., *Colloid. Surface. A.* 229-242 (2002) 207

[4] I. Armentano, et al., *Polym. Degrad. Stab.* 2126-2146 (2010) 95

[5] C. Vaquette, et al., *Mendeleev Commun.* 38-41 (2008) 18

## **Kseniia N. Grafaskaia**

[kseniya.grafskaya@phystech.edu](mailto:kseniya.grafskaya@phystech.edu)

Moscow Institute of Physics and Technology (State University)

**PhD student**

9 Institutskiy per., Dolgoprudny, Moscow Region, 141700, Russia

**Research interests:** polymer science, investigation of different properties of liquid-crystalline structures, experiment designing, computer simulations and calculations



### **SAXS analysis of the lyotropic phase formation in self-assemble systems**

One of the promising ways toward the development of renewable power sources is the improvement of the modern ion-exchange membrane performance. [1,2] Nowadays the most efficient way to design ion-selective membrane is based on molecular self-assembly. [3]

Our group pursued an approach, [4] where fabrication of ion-exchange membranes have been performed via the supramolecular assembly of low-molecular-weight wedge-shaped amphiphiles. One of their features is to form supramolecular structures with different phases. [5,6,7] During exposure to humid atmosphere the system resulting in the formation of a lyotropic phase. It should be mentioned that ion channels organized in such systems that can be arrested by photo-polymerization. Thus, nanostructured polymer membranes with a long-range order can be obtained. Such handling allows a cut above control over the ion channel size, topology and structure.

In continuation of our previous work, we employ the molecules bearing sulfonate groups at the tip of the wedge and a hydrophobic tail at the periphery. Small-angle X-ray scattering (SAXS), are employed for the structure investigation into fibers of such compounds. In addition, to fit the experimental SAXS data we employed several structural models. It allows us to perform the detailed structural analysis beyond the simple phase identification.[8] By using simple computed models for the SAXS analysis one can obtain significant insights into the micro-structure of the amphiphilic mesogens during swelling process. Results show that not only water uptake effect on the ion channel size but also the molecular architecture. For example, structure of the rigid molecular fragment bearing a polar group can limit the ion channel dimensions.[9] These findings can be used for the ion transport optimizing and moreover for development of efficient ion-selective membranes.

This work was financially supported by the Russian Science Foundation (project no. № 16-13-10369).

- [1] M. O'Neill and S. M. Kelly, *Adv. Mater.* 1135–1146 (2003) 15.
- [2] H. Shimura, et al., *J. Am. Chem. Soc.* 1759–1765 (2008) 130.
- [3] N. Li and M. D. Guiver, *Macromolecules* 2175–2198 (2014) 47.
- [4] H. Zhang, et al., *Adv. Mater.* 3543–3548 (2013) 25.
- [5] Y. Chen, et al., *J. Phys. Chem. B* 3207–3217 (2014) 118.
- [6] J. Lejnieks, et al., *ChemPhysChem* 3638–3644 (2010) 11.
- [7] K. Grafaskaia, et al., *AIP Conf. Proc.* 04009 (2016) 1748.
- [8] A. Sundblom, et al., *J. Phys. Chem. C* 7706–7713 (2009) 113.
- [9] K.N. Grafaskaia, et al., *Phys. Chem. Chem. Phys.* 30240-30247 (2015) 17.

## **Jan Gruenert**

[jan.gruenert@xfel.eu](mailto:jan.gruenert@xfel.eu)

European XFEL

### **Group Leader X-ray Photon Diagnostics**

European XFEL GmbH, Holzkoppel 4, 22869 Schenefeld, Germany

X-ray photon diagnostics

**Research interests:** Large scale photon facilities – design, installation, operation Ultrafast laser optics (for temporal diagnostics)



## **Tunnel installation of the European XFEL Photon Diagnostics**

The European X-ray Free-Electron-Laser (XFEL.EU) is a 4<sup>th</sup> generation light source, which will deliver X-ray pulses with femtosecond duration and sub-Ångström wavelength at MHz repetition rates. This new facility is currently under construction in the Hamburg metropolitan area in Germany and is scheduled to come into operation in 2017. Special diagnostics [1,2] for spontaneous radiation analysis is required to tune the machine into the lasing condition. Once lasing is achieved, diagnostic imagers [3], online monitors [4], and the photon beam transport system [5] will have to cope with extreme radiation intensities. The installation and technical commissioning of machine equipment in the photon area of the facility is in full swing. This contribution presents an overview of photon diagnostics devices, the progress on their final assemblies and focuses on describing their installation in the tunnels.

- [1] J. Grünert, “Conceptual Design Report: Framework for X-Ray Photon Diagnostics at the European XFEL”, XFEL.EU technical report TR-2012-003, April 2012
- [2] W. Freund, “The Undulator Commissioning Spectrometer for the European XFEL”, DESY-2014-03060, XFEL.EU TN-2014-001-01
- [3] A. Koch et al., “Design and initial characterization of x-ray beam diagnostic imagers for the European XFEL”, Proc. SPIE 9512, Advances in X-ray Free-Electron Lasers Instrumentation III, 95121R (May 12, 2015); doi:10.1117/12.2182463
- [4] J. Buck et al., “Time-of-flight photoemission spectroscopy from rare gases for non-invasive, pulse-to-pulse X-ray photon diagnostics at the European XFEL”, Proc. SPIE 8504, X-Ray Free-Electron Lasers: Beam Diagnostics, Beamline Instrumentation, and Applications, 85040U (October 15, 2012); doi:10.1117/12.929805
- [5] H.Sinn et al., “Technical Design Report: X-Ray Optics and Beam Transport”, December 2012, XFEL.EU TR-2012-006, doi:10.3204/XFEL.EU/TR-2012-006

## Ekaterina Iashina

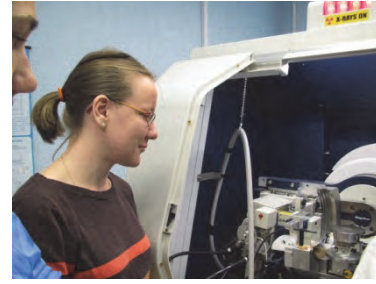
yashina\_91@inbox.ru

Petersburg Nuclear Physics Institute NRC KI

Research laboratory assistant

Gatchina, 188300 St-Petersburg, Russia

Research interests: Small-angle neutron scattering



### Project of the ultra small-angle neutron scattering setup SESANS for the instrument base at the PIK reactor

Spin-echo small-angle (SESANS) technique is a new efficient method to measure structures of materials in real space. The SESANS approach links the polarization  $P(z)$  of the neutron beam to the projection  $G(z)$  of the autocorrelation function  $\gamma(r)$  of the density distribution  $\rho(r)$  of the sample. The method is based on the Larmor precession of polarized neutrons transmitted across two precession devices before and after the sample, which encodes the scattering angle into a precession angle [1]. The polarization in a SESANS experiment is measured as a function of the total scattering cross section  $\sigma$ , the thickness of the sample  $l$  and the spin-echo length  $z$

$$P(z) = \exp(l \sigma (G(z)-1)). \quad (1)$$

The technique allows to measure a full correlation function in samples over distances from 20 nm to 20 mkm. The ability to measure the correlation at a micron scale is an incredibly important to study of biological cells. Chicken erythrocyte nuclei was studied

at the SESANS instrument at the TU Delft (Fig. 1). The instrument at the TU Delft uses a constant wavelength  $\lambda = 2 \text{ \AA}$ .

The measurements were carried out in solution of  $D_2O >95\%$  to reach the maximum contrast for the scattering. Three different thickness of the sample (2, 4, 10 mm) were used to obtain the noticeable SESANS signal from the chromatin in the nucleus. The noticeable function had been measured for the sample of 10 mm only.

As it is impossible to increase the thickness of the specimen to infinity, one should change the other parameter,  $\sigma$ , which can be easily done via variation of the neutron wavelength

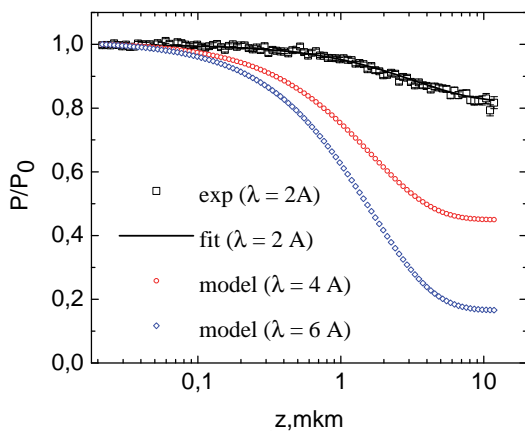


Fig.1 The polarization from isolated chicken erythrocyte nuclei as function of the spin-echo length  $z$  is shown with different wavelength.

$\lambda$ .

The simple calculations show that the use of the beam with the  $\lambda=6\text{\AA}$  leads to increase of the sensitivity of the method and open the range of  $z$  [0.1 - 1.0] mkm for the study of biological cells (Fig. 1).

We propose the SESANS setup with the changeable wavelength in the range from 2 to 10  $\text{\AA}$  for the instrument base at the PIK reactor at the Petersburg Nuclear Physics Institute of NRC Kurchatov Institute.

[1] M. Theo Rekveldt, Nuclear Instruments and Methods in Physics Research B 114 (1996) 366-370

## **Kseniia Ilina**

[Ilina-ks@mail.ru](mailto:Ilina-ks@mail.ru)

Federal Scientific Research Centre “Crystallography and Photonics” of  
Russian Academy of Sciences

**Junior research scientist**

119333, Russia, Moscow, Leninsky pr., 59

**Research interests:** Protein crystallization, thin films physics,  
Langmuir-Blodgett technique, surfaces and interfaces, crystal structure  
defects, research methods of crystal structure, molecular modelling  
techniques



### **Investigation of the preliminary crystallization stage in lysozyme solutions by small-angle x-ray scattering.**

Crystallization of proteins is a promising scientific field. Today there is a problem to find the proteins crystallization conditions. There is no exact algorithms of crystallization, because the protein crystals growth is a complex physical-chemical process that depends on many different factors: pH, temperature, concentration of the crystallization solution components, composition of solutions [1-3]. Usually during the searching of conditions an enumeration of various conditions occurs. Protein crystallization mechanisms are little studied, it is not known, how the protein crystals growth and which units are involved in the crystal growth. We suggested that certain oligomers are crystal growth units. For experimental confirmation of our hypothesis we investigated the protein lysozyme solution in the initial crystallization stage by small-angle X-ray scattering (SAXS).

The first part of the work was determination of the growth units on the base of the Structural analysis of tetragonal lysozyme (PDB ID: 4WLD). The analysis of the crystalline molecular packing of tetragonal lysozyme showed, that there were repeated motifs in the structure which could be assembled by translating. Two types octamers were allocated by analyzing of the crystalline molecular packing. Octamers, hexamers, tetramers, and dimers were modeled with *Coot* and PyMOL programs [4]. In the second part of this work we investigated the protein solutions by small-angle X-ray scattering at optimal crystallization conditions and in the absence of crystallization to find the oligomers in solution. Monitoring of the crystallization process was carried out by temperature changing. SAXS experiments were performed on the DICSY synchrotron beamline (NRC Kurchatov Institute, Moscow). It was shown that monomers, dimers and octamers appear in solution under optimal crystallization conditions of tetragonal lysozyme. And there are only monomers in solution under the crystallization conditions when no crystal growths. According to the data, we suggest that octamers are growth units of the tetragonal lysozyme [5].

- [1] Ries-Kautt M.M., Ducruix A.F. // J. Biol. Chem. 1989. V. 264. № 2. P. 745.
- [2] Kam Z., Shore H.B., Feher G. // J. Mol. Biol. 1978. V. 123. № 4. P. 539.
- [3] Pusey M.L., Snyder R.S. // J. Biol. Chem. 1986. V. 261. № 14. P. 6524.
- [4] Schrodinger, LLC, The PyMOL Molecular Graphics System, Version 1.3r1. In ed.; 2010
- [5] Kovalchuk M.V., Blagov A.E., Dyakova Yu.A., Gruzinov A.Yu., Marchenkova M.A., Peters G.S., Pisarevsky Yu.V., Timofeev V.I., Volkov V.V. // Cryst. Growth Des. 2016. V. 16. P. 1792–1797.

## **Nikolay Kameko**

[Kamekework@rambler.ru](mailto:Kamekework@rambler.ru)

M.V.Lomonosov Moscow State University

**Scientist**

Leninskie Gory, Moscow 119991 Russia

**Research interests:** Vacuum ultraviolet spectroscopy of solids using synchrotron radiation, photoelectron spectroscopy, nanocrystals



### **Photoelectron spectroscopy of silicon nanocrystals in insulating matrices**

The structure, optical and luminescence properties of oxide, oxynitride and nitride superlattices formed by PECVD deposition of alternating layers of  $\text{SiO}_x/\text{SiO}_2$  in case of oxide samples or  $\text{SiN}_x/\text{Si}_3\text{N}_4$  in case of nitride ones were studied by a variety of techniques. Creation of silicon nanocrystals after annealing was confirmed by GIXRD for all the samples studied. Layered structure as a function of the thickness of barrier and active layers was verified by X-ray reflectivity. After that the samples were studied by PES (ESCHA). To investigate PES spectra at different depths the surface of the samples was etched by the bombardment by argon ions.

PES spectra reveal the presence of covalent bonds Si-Si ( $\text{Si}^0$  valent state), ionic bonds in  $\text{SiO}_2$  ( $\text{Si}^{4+}$  valent state) as well as the presence of suboxides  $\text{SiO}_x$  ( $0 < x < 2$ ) in all such superlattices. The spectra allow to evaluate the portion of silicon nanoclusters. Charging of the samples under irradiation was observed, which decreased after etching. Evolution of PES spectra is discussed. The processes of energy transfer and photon multiplication under high energy excitation are considered.

Financial support of the RF Ministry of Science and Education grant under the agreement RFMEFI61614X0006 is gratefully acknowledged.

## Fedor Kashaev

[kashaev.fedor@gmail.com](mailto:kashaev.fedor@gmail.com)

Lomonosov Moscow State University

PhD Student

1/2 Leninskie Gory, Moscow, 119991, Russia

**Research interests:** Laser ablation, femtosecond laser pulses, nanostructuring, silicon nanoparticles, bioimaging, atomic-force microscopy, Raman scattering, photoluminescence



### Structural and optical properties of nanoparticles formed via laser ablation of porous silicon in gases and liquids

One of the most promising methods for producing nanostructures is a laser ablation of the solid surface, characterized by low content of undesired impurities. Femtosecond laser ablation of porous medium is of great interest due to increase in these media as linear-optical effects, such as the enhancement of the Raman scattering efficiency [1]; as non-linear-optical effects, for example the enhancement of the cubic nonlinear susceptibility [2]. The nanoparticles, formed at these conditions can be used for potential applications in biomedical field as contrasting agents in optical coherence tomography [3] due to biocompatibility and biodegradability of silicon nanoparticles.

This work presents results of experiments of the nanoparticle formation as a result of ultrafast laser ablation of porous silicon in water and helium. During the experiment the target was irradiated with Cr:forsterite femtosecond (1250 nm, 180 fs, 10 Hz, 10 J/cm<sup>2</sup>) and Nd:YAG picosecond (1064 nm, 30 ps, 10 Hz, 7 J/cm<sup>2</sup>) laser pulses at room temperature. The choice of porous silicon as a material for experiments is caused by a lower threshold of ablation in comparison with crystalline silicon. During the ablation of the crystalline silicon ablation threshold is equal to 1 J/cm<sup>2</sup>, whereas for porous materials threshold equals 0,1 J/cm<sup>2</sup>. This feature leads to a greater exit of substance at lower energy costs at a case of ablation of porous silicon.

Determination of the structural properties of the formed samples is important due its influence on optical and electrical properties of the particles. The size of nanoparticles fabricated via laser ablation was determined by atomic-force microscopy (AFM) and ranges from 10 to 60 nm. The samples with minimum size of nanostructures was obtained at a case of ablation in helium at pressure 500 mbar (Fig.1)

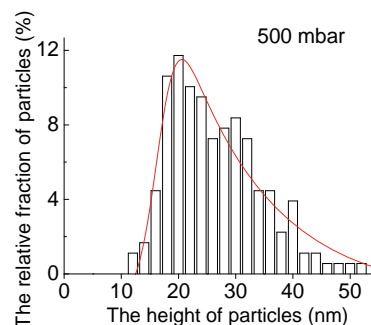


Fig.1 Particle size distribution of silicon nanoparticles, formed by means of the fs laser ablation of por-Si in helium at pressure 700mbar.

By means of a Raman scattering spectroscopy the phase structure of the created nanoparticles was defined. Besides structural properties, optical properties were also investigated.

[1] L.A. Osminkina, et al., *Nanoscale Research Letters* 524-529 (2012) 7

[2] V.Ya. Gayvoronsky, et al., *Quantum Electronics* 257-261 (2011) 41

[3] M.Yu. Kirillin, et al., *Laser Phys.* 075604(1) -075604(7) (2015) 25

## **Julia K. Keppler**

[jkeppler@foodtech.uni-kiel.de](mailto:jkeppler@foodtech.uni-kiel.de)

Division of Food Technology, Kiel University

**Post doc**

Heinrich-Hecht Platz 10, 24118 Kiel, Germany

**Research interests:** Protein-ligand interactions Protein conformation and aggregation Disperse systems and interface structure



### **Binding of (-)-epigallocatechin gallate to different genetic variants of dimeric whey protein beta-lactoglobulin**

#### **Introduction**

The whey protein beta-Lactoglobulin (BLG) can interact non-covalently with small hydrophobic ligands such as polyphenol (-)-epigallocatechingallate (EGCG) and act as natural transporter in a hydrophobic environment. This is especially interesting for application in functional foods, as the protein-polyphenol interaction was found to prevent oxidation of the polyphenol and reduced the bitterness perception [1]. BLG exists in several different genetic variants of which A and B are most common. At physiological conditions the protein is reported to dimerize – resulting in AA, BB (homodimers) or AB dimers (heterodimers). Although the protein and its binding to small molecules is intensely characterised, the interaction of ligands like EGCG with hetero and homodimers is largely unknown. For food technological purposes it is interesting to analyse, if hetero or homodimers differ in their transport capacity as both dimer types can be specifically used for such an application. In general the different binding behaviour could also occur in other genetic variants of lipocalin proteins – some of which are important transport proteins in the human body.

#### **Material & methods**

Interaction (number of binding sites and conformational changes) of EGCG with heterodimers and homodimers was analysed using fluorescence quenching and FT-IR. Aggregation was analysed using DLS and SAXS.

#### **Results & discussion**

The present findings revealed that EGCG interacts significantly different with hetero and homodimers of BLG in the order BLG AA > BB > AB: BLG homodimers AA and BB possess approximately one additional binding site for EGCG (n= 2 binding sites) compared to heterodimer AB (n = 1 binding site). Conformational changes detected with FT-IR also confirmed a stronger interaction of homodimers compared to heterodimers. Further, aggregation after addition of EGCG as detected by SAXS is in the order AA (20 – 50 monomers) > BB (13-30 monomers) > AB (4-10 monomers).

In summary BLG homodimer AA shows significantly stronger reaction towards EGCG than the more common BLG AB heterodimer. With regard to delivery systems for food applications the AA genetic protein variants seems superior. The results suggest that genetic variability could also significantly influence the transport properties of other lipocalins – depending on the ligand.

- [1] A. Shpigelman, Y. Cohen, Y.D. Livney, Thermally-induced  $\beta$ -lactoglobulin-EGCG nanovehicles: Loading, stability, sensory and digestive-release study, *Food Hydrocolloids* 29 (2012) 57–67.

**Aleksandr Klyuyev**

[rinaskela@gmail.com](mailto:rinaskela@gmail.com)

Belgorod State National Research University

**Master student**

85, Pobedy St., Belgorod, 308015, Russia

**Research interests:** Physics of interaction ionizing radiation with matter



## **Observation the diffraction peculiarities of real and virtual photons in powders**

The Coulomb field of a charged particle can be considered as a field of virtual photons. Parametric X-ray radiation (PXR) appears due to a virtual photons diffraction on atomic structures. PXR is well studied both theoretically and experimentally in a wide range of energies of emitting charged particles and for different media (crystals, polycrystals, multilayer mirrors). Unlike wideband X-ray, which is formed along the extinction length, PXR is formed on the photoabsorption length. This peculiarity is one of the main differences in diffraction processes of real and virtual photons. The experimental study of PXR generated by relativistic electrons interacting with diamond powders is presented and differences between diffraction processes of real and virtual fields are shown.

The spectra measured under interaction of the 7 MeV electron beam with different grain sizes diamond powders (60/40, 7/5 and 0.5/0 mkm) allowed to observe differences between formation lengths of PXR and X-ray diffraction. The measurements were performed by semiconductor detectors at the observation angles of 150 and 180 degrees relative to electron beam propagation direction. The measurements of the diffracted X-rays were made for the observation angle 150 degrees for the case of an electron beam was exchanged by the collimated wide band X-ray flux generated with X-ray tube.

The results show the different dependences of the measured spectra on the grain sizes of used powders for diffraction of virtual and real photons.

This work was supported by grant 16-32-00502 мол\_a from the Russian Foundation for Basic Research.

**Irina Kolesnikova**

[varsharova@mail.ru](mailto:varsharova@mail.ru)

LFE of Tomsk State University

**Junior research scientist**

Russian Federation, Tomsk, Fedora Lytkina str. 28g

**Research interests:** x-ray detectors, photonics, nonlinear dynamics



## **Electrophysical and optical properties of GaAs:Cr**

The report presents the results of experimental studies of the electrical characteristics of 3-inch wafers of a high-resistance (HR) GaAs:Cr and the characteristics of sensors based on it. Resistivity distribution was obtained by analyzing the current-voltage characteristics and using the contactless resistivity mapping method. It is shown that the distribution of the resistivity across the wafer surface is determined by the original distribution of impurities and the temperature at which the chromium diffusion was carried out.

The distribution of intensity across the thickness of samples was investigated using the Pockels effect. As objects of study HR GaAs pad sensors with an area of 0.2 - 0.25 cm and the thickness of the sensitive layer in the range of 450-650 microns were used. Metal contacts were fabricated by chemical deposition of nickel (Ni) with thickness of 0.5 - 1 micron or by electron-beam sputtering of Cr / Ni film with a total thickness of 0.1 - 0.2 micron on both sides of pad sensor. Therefore, sensors have «Ni - HR GaAs - Ni» symmetrical structure or «Ni / Cr - HR GaAs - Cr / Ni» structure.

The distribution of the intensity at voltage 800 V on SI LEC GaAs: EL2 pad sensor shown at figure 1.a). The distribution of the intensity at voltage 800 V on HR-GaAs:Cr pad sensor shown at figure 1.b).

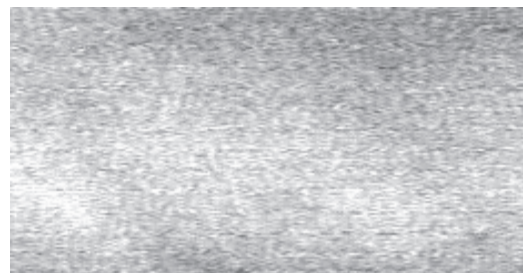


Figure 1. The intensity distribution of the infrared radiation passing across the volume of  
a) SI LEC GaAs: EL2 pad sensor      b) HR-GaAs:Cr pad sensor.

The thickness of the active region is dependent on the voltage on the sensor with a coefficient of 1 micron / V. The strong field represented by the bright areas on the image. This demonstrates the effective absorption of infrared radiation on EL2 centers due to the localization of an electric field in a relatively narrow area. In addition, there are fluctuations of the electric field with time, resulting in current oscillations in the external circuit. It was established experimentally that in the HR GaAs sensors field distribution significantly more uniform compared to sensors based on the SI GaAs: EL2. It is shown that the HR GaAs sensors have no temporary fluctuations in the electric field.

## Nickolay Kolyshkin

[nickelprog@mail.ru](mailto:nickelprog@mail.ru)

National Research Centre "Kurchatov Institute"

Research engineer

1 Akademika Kurchatova pl., 123182 Moscow (Russia)

Research interests: X-ray diffraction



### Resonant diffraction calculations for fluorite-pyrochlore phase transition study in $\text{Eu}_2\text{Hf}_2\text{O}_7$

N.A. Kolyshkin<sup>1</sup>, A.A. Veligzhanin<sup>1</sup>, Y.V. Zubavichus<sup>1</sup>, V.V. Popov<sup>1,2</sup>

<sup>1</sup>National Research Center "Kurchatov Institute", Moscow, Russia

<sup>2</sup>National Research Nuclear University "MEPhI", Moscow, Russia

$\text{Eu}_2\text{Hf}_2\text{O}_7$  belongs to a wide class of complex oxides with the chemical formula  $\text{Ln}_2\text{M}_2\text{O}_7$ . This oxide has structure of either the fluorite- (Fm-3m) or the pyrochlore- (Fd-3m) type depending on the synthesis temperature. Fluorite-pyrochlore transition that occurs with increase of synthesis temperature is accompanied by cation and anion ordering. However, it's difficult to examine this transition using ordinary X-ray diffraction due to proximity of atom scattering factors for europium ( $Z=63$ ) and hafnium ( $Z=72$ ).

Anomalous (or resonant) X-ray diffraction (AXRD) is a method of the X-ray scattering where the energy of incident radiation is relatively close to the absorption edge of one of the elements the studied substance includes. The scattering factor of this element significantly varies so the intensities of diffraction reflexes in certain cases can grow.

For the phase transition analysis there was made calculations of resonant diffraction for  $\text{Eu}_2\text{Hf}_2\text{O}_7$  at the L3-edge of hafnium.  $I_{\text{calc}}(E, hkl)$  intensity spectra were calculated by ad hoc program with a variation of three structural parameters. These parameters correspond to the Hf and Eu cations ordering, the concentration of oxygen in the 8a position and the free coordinate of the oxygen in 48f position, so they can qualify the transition fluorite  $\rightarrow$  pyrochlore. Calculated  $I_{\text{calc}}(E, hkl)$  spectra were compared to the experimentally measured on the "Structural Materials" beamline of the Kurchatov synchrotron radiation source and showed semiquantitative agreement. Estimation of the structural parameters indicates a mixture of fluorite and pyrochlore oxide phases in the studied material.

## Artem Korshunov

[artem.korshunov91@gmail.com](mailto:artem.korshunov91@gmail.com)

Petersburg Nuclear Physics Institute

Research laboratory assistant

Orlova Roscha, Gatchina, Leningrad district, 188300, Russia

**Research interests:** neutron powder diffraction, development and study of new materials, structural analysis



### Study of the spin structure of honeycomb layered compound $\text{Li}_3\text{Ni}_2\text{SbO}_6$ antimonate

Design and synthesis of new layered oxides of alkali and transition metals as perspective materials of solid electrolytes or electrode materials, led to the discovery of the existence of unique, very useful and promising physical properties in terms of their application. Currently, the actual problem is to investigate magnetic properties of these compounds, which associated with a change of transition metals valence and spin states and come out among ionic transfer processes and different types of magnetic ordering. Study of the spin structure of  $\text{Li}_3\text{Ni}_2\text{SbO}_6$  antimonate and its temperature evolution by neutron powder diffraction has been carried out within the scope of this research.

$\text{Li}_3\text{Ni}_2\text{SbO}_6$  sample was prepared by conventional solid-state reactions at 980–1030 °C followed by quenching as described in [1]. A part of this sample was used for the measurements of temperature dependence of the magnetic susceptibility, specific heat, magnetization, electron spin resonance and nuclear magnetic resonance [2].

Low-temperature neutron diffraction experiments were carried out on the cold neutron two-axis diffractometer G4.1 located at ORPHEE reactor, Laboratory Léon Brillouin, Saclay, France.  $\lambda=2.422$  Å. Neutron diffraction data was measured in the angular range of  $2\theta$ : 11-91 degrees with step size of  $0.1^\circ$ . Additional reflexes, associated with magnetic scattering of neutrons, appear at temperatures below 15 K, which is in agreement with the data for magnetic susceptibility

As a result of the profile analysis of the diffraction pattern of  $\text{Li}_3\text{Ni}_2\text{SbO}_6$  measured at  $T = 1.5$  K, it was discovered that the magnetic structure is commensurate and can be described with the propagation vector  $\mathbf{k} = (1/2 \ 1/2 \ 0)$ . This structure can be considered as zigzag ferromagnetic chains coupled antiferromagnetically. Obtained magnetic moment is equal to  $1.62(2) \mu_B/\text{Ni}$ .

It should be noted that this model of spin ordering is in good agreement with theoretical calculations based on density functional theory, which shows that both ferromagnetic and antiferromagnetic spin exchange interactions between  $\text{Ni}^{2+}$  ions are present in the honeycomb planes, keeping a zigzag antiferromagnetic ground state [2]. The theoretical calculations show that interplane exchange coupling is very weak, so that  $\text{Li}_3\text{Ni}_2\text{SbO}_6$  antimonate can be considered as 2D magnet.

This work was supported by the Russian Foundation for basic Research (project 16-02-00360).

[1] V. V. Politaev, et.al., J. Solid State Chem., 183, 684, 2010

[2] E.A. Zvereva, et.al., Phys. Rev. B 92, 144401 (2015)

## **Ksenia Kozlovskaya**

[kozlovskaya@physics.msu.ru](mailto:kozlovskaya@physics.msu.ru)

M.V.Lomonosov MSU Faculty of Physics,

**Researcher**

1/2 Leninskie Gory, Moscow, 119991, Russia

**Research interests:** X-ray scattering, X-ray absorption spectroscopy,  
Synchrotron radiation



### **Absolute atomic configuration of chiral crystals: a novel solution**

**Ksenia Kozlovskaya**<sup>1</sup>, V.Dmitrienko<sup>2</sup>, E.Ovtchinnikova<sup>1</sup>, J.Kokubun<sup>3</sup>, A.Rogalev<sup>4</sup>

<sup>1</sup> M.V.Lomonosov MSU Faculty of Physics, Moscow, Russia. <sup>2</sup> Shubnikov Institute of Crystallography, Moscow, Russia, <sup>3</sup> Faculty of Science and Technology, Tokyo University of Science, Japan <sup>4</sup> ESRF, Grenoble, France

The majority of known crystals are chiral and may exist in the right or left configurations related by inversion. For many applications one should know the absolute atomic structure of chiral crystals. X-Ray methods used to distinguish right and left configurations are based on anomalous x-ray diffraction on heavy metals nuclei [1, 2]. But if a crystal consists of light atoms or all atoms in a crystal are the same, we need a new way.

We propose a new method to determine the absolute configuration of any crystals, based on the azimuthal asymmetry of multiple scattering. In the X-ray scattering the intensity of each reflection is composed of intensities of the main two-wave reflection and a variety of three-wave (renninger's) contributions. The main contribution is not sensitive to the chirality and does not change when the crystal rotates around the azimuthal axis because of Friedel law:  $|F(hkl)| = |F(-h-k-l)|$ . But three-wave contributions are sensitive to chirality and do not rely on the imaginary parts of atomic scattering factors, and the azimuthal dependence of their intensity is different for the right and left configurations.

Thus, in order to distinguish right and left crystal configurations, it is necessary to measure the three-wave azimuthal dependence and compare it with the theoretical calculations, which are all reliable and model independent. Measurements with circular polarized X-ray radiation are available now at the modern synchrotrons and can be realized at the “forbidden” Bragg reflections which do not contain strong two-wave contributions.

The efficiency of this method was checked during the experiment on the ESRF's ID12 beamline. We have studied the right-handed and left-handed samples of SiO<sub>2</sub> (quartz, space groups P3121 and P3221) and measured the azimuthal Renninger plots for the forbidden 001 reflection with the right and left circular polarizations of incident radiation. So we obtain the chiral asymmetry ratio  $(I_{\text{left}} - I_{\text{right}}) / (I_{\text{left}} + I_{\text{right}})$  as function of azimuthal angle. To exclude resonant contributions, we have choosed the beam energy 4.5 KeV (far from the absorption edges of Si and O). The measured azimuthal dependence of the asymmetry ratio is different for the right-handed and left-handed quartz in consistence with theoretical prediction and allows to find out the absolute atomic configuration of each sample.

[1] J.M. Bijvoet, A.F. Peerdeman, A.J. Van Bommel, Nature **168** (4268): 271-273 (1951).

[2] H. D. Flack, Acta Crys., **A39**: 876 881 (1983).

## **Elena Kuchma**

[elenaku4ma@yandex.ru](mailto:elenaku4ma@yandex.ru)

Smart Materials International Research Center

Southern Federal University

**Master student**

344090 Russia, Rostov-on-Don, Sladkova 178/24

**Research interests:** Nanomaterials for bio-medical applications

Synchrotron radiation



### **Superparamagnetic Colloidal Nanoparticles for Theranostics in Oncology**

Nanomedicine has become nowadays one of the most important research fields [1]. Further development of novel advanced nanomaterials for biomedical applications is limited to great extent by the lack of cutting-edge characterization techniques of both nanoparticles themselves and their spatial distribution in biological tissues after administration. Magnetic nanoparticles for theranostics application in oncology (contrast agent for MRI (Magnetic Resonance Imaging) and active material for Magnetic Hyperthermia treatment) should be optimized in size, shape (and corresponding surface chemistry) and specific magnetic characteristics. A possibility of fine tuning of these nanoparticles characteristics could be a very important step towards personalized nanomedicine.

Iron oxide based colloidal magnetic nanoparticles are promising candidates for theranostics in oncology as one could use them both for diagnostics (as a contrast agent in MRI [2]) and simultaneously for therapy (as active agent for magnetic hyperthermia of tumour tissues [3]). Using advanced micro-wavy synthesis technique we manufactured colloidal magnetic nanoparticles having tuneable magnetic and biochemical properties, thus, preparing a base for a future personalized nanomedicine platform. To get detailed insight into the relationships between parameters of colloidal magnetic nanoparticles such as size, morphology (shape and atomic structure), stoichiometry, type of surfactant covering the nanoparticles and obtained magnetic and biochemical properties of the superparamagnetic iron oxide based colloidal magnetic nanoparticles advanced in-situ x-ray spectroscopic methods were applied. Till now most x-ray spectroscopic characterizations of magnetic nanoparticles for bio-medical applications are not performed in their natural colloidal form, but in powder (solid state) form. In the present study advanced x-ray spectroscopies were used for in-situ study of colloidal magnetic nanoparticles in solution form, reproducing their “natural” conditions in biological tissues. High-resolution XANES [4] and non-resonant XES [5] at ID26 beamline of ESRF were applied to study the electronic structure of the colloidal nanoparticles in both occupied and unoccupied electronic states regions. High energy resolution XAFS, obtained through selective fluorescence detection with the following advanced FitIt [6] theoretical treatment was used to obtain the 3D local structure parameters exploiting the improved full-potential FDMNES code [7].

- [1] Fuyao Liu et al, Nature Communications 6 (2015) 6: 8003.
- [2] Forrest M. Kievit and Miqin Zhang, Acc. Chem. Res., 44 (2011) 853–862.
- [3] Jae-Hyun Lee et al. Nature Nanotechnology 6 (2011)418–422.
- [4] Glatzel et al. J. Electron. Spectr. Rel. Phenom. 188 (2013)17-25
- [5] Sikora et al. Phys. Rev. Lett. 105 (2010) 037202; Juhin et al. Nanoscale 6 (2014) 11911
- [6] G. Smolentsev, A. V. Soldatov, Computational Materials Science 39 (2007) 569.
- [7] S. A. Guda, et al., J. Chem. Theory and Comput., 11 (2015) 4512-4521

## Elena Kuznetsova

[e.kuznetsova@inorg.chem.msu.ru](mailto:e.kuznetsova@inorg.chem.msu.ru), [kuznetsova.chemmsu@yandex.ru](mailto:kuznetsova.chemmsu@yandex.ru)

Lomonosov Moscow State University, Department of Chemistry,  
Inorganic Chemistry Division

### PhD student

1 building 3 Leninskie Gory, 119991 Moscow, Russia

**Research interests:** inorganic chemistry, solid state physics, selenites,  
low-dimensional magnetism, crystallography, X-ray diffraction



## Synthesis, structure and magnetic properties of francisite family compounds

### $\text{Cu}_3\text{M}(\text{SeO}_3)_2\text{O}_2\text{Cl}$ (M = Y, La, Pr, Nd, Sm, Eu, Gd, Dy, Ho, Er, Yb, Lu)

Mineral francisite  $\text{Cu}_3\text{Bi}(\text{SeO}_3)_2\text{O}_2\text{Cl}$  is characterized by the rare combination of chemical elements met in this fine mineral only [1]. It was shown that Bi can be substituted by Y or lanthanide, thus resulting in the formation of francisite family of compounds. This family of compounds is a good example of a situation where correlations between composition, crystal structure and physical properties can be observed and evaluated experimentally. All compounds of this family reach long-range ordered antiferromagnetic state at low temperatures and exhibit field-induced metamagnetic transition prior to full saturation in moderate magnetic field [2].

The magnetic structure of francisite was found to be far from the simple collinear one being governed by multiple competing superexchange interactions. In fact, the neutron scattering study has revealed the six sub-lattices canted antiferromagnetic structure quite sensitive to an external magnetic field [3, 4]. Besides, the magnetic response of both  $\text{Cu}_3\text{Bi}(\text{SeO}_3)_2\text{O}_2\text{Cl}$  and  $\text{Cu}_3\text{Bi}(\text{SeO}_3)_2\text{O}_2\text{Br}$  was found to be rather anisotropic. From the density-functional band structure calculations, it was shown that the description of francisite's ground state must include microscopic Dzyaloshinskii-Moriya interactions and it was stressed that the features of the magnetization process deserve further experimental investigation of these compounds [5]. Systematically, this investigation can be done on Ln substituted francisites owing to the fact that the full row of rare earth compounds is available for experimental study [6]. It should be noted, however, that the presence of lanthanides in the francisite's structure makes its magnetic response significantly more complicated, in part due to the complex interplay of rare earth and transition metal anisotropies. The complications can be avoided in cases of nonmagnetic trivalent Ln metals, i.e. La, Eu and Lu.

In this study synthesis, crystal structure and magnetic properties of  $\text{Cu}_3\text{M}(\text{SeO}_3)_2\text{O}_2\text{Cl}$  (M = Y, La, Pr, Nd, Sm, Eu, Gd, Dy, Ho, Er, Yb, Lu) are presented. Interrelation between chemical composition and magnetic behavior of francisite-like compounds is discussed.

This study was supported by RFBR grant №14-03-00604.

- [1] A. Pring, B.M. Gatehouse, W.D. Birch, *Amer. Mineral.* 75 (1990) 1421-1425
- [2] P. Millet, B. Bastide, V. Pashchenko, S. Gnatchenko, V. Gapon, Y. Ksari, A. Stepanov, J. Mater. Chem. 11 (2001) 1152-1157.
- [3] K.V. Zakharov, E.A. Zvereva, P.S. Berdonosov, E.S. Kuznetsova, V.A. Dolgikh, L. Clark, C. Black, P. Lightfoot, W. Kockelmann, Z.V. Pchelkina, S.V. Streltsov, O.S. Volkova, A.N. Vasiliev, *Phys. Rev. B.* 90 (2014) 214417.
- [4] M. Pregelj, O. Zaharko, A. Gunther, A. Loidl, V. Tsurkan, S. Guerrero, *Phys. Rev. B.* 86 (2012) 144409.
- [5] I. Rousochatzakis, J. Richter, R. Zinke, A.A. Tsirlin, *Phys. Rev. B.* 91 (2015) 024416.
- [6] P.S. Berdonosov, V.A. Dolgikh, *Russ. J. Inorg. Chem.* 53 (2008) 1353- 1358.

## Charlotte Lorenz

[c.lorenz@fz-juelich.de](mailto:c.lorenz@fz-juelich.de)

Juelich Centre for Neutron Science (JCNS-1)

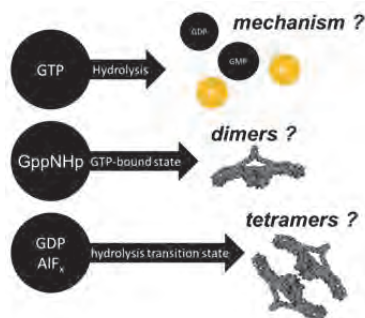
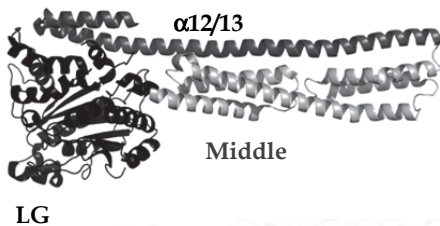
PhD student

Forschungszentrum Juelich, 52425 Juelich, Germany

**Research interests:** Small Angle Scattering, Structure modelling, Proteins



### Caught in the act – studies of hGBP1 polymerization



The human Guanylate Binding Protein 1 (hGBP1) hydrolyzes guanosine triphosphate (GTP) to produce GDP, GMP and free phosphate in an exergonic reaction. It belongs to the family of dynamin-like proteins where some family members are known to use this free energy to undergo conformational changes and exhibit mechanical force. [1, 2] hGBP1 is regulated by presence of nucleotides: GTP binding initiates an interaction between the LG domains leading to dimerization. Further oligomerization to tetramers is proposed to take place during hydrolysis. [1, 3, 4, 5] This reaction cycle can be studied in the presence of non-hydrolyzable nucleotides like GppNHp to characterize the GTP-bound oligomeric state and in presence of GDP and aluminium fluoride ( $\text{AlF}_x$ ) to mimic the transition state during hydrolysis. [2]

The oligomeric state was determined in previous experiments based on hydrodynamic radius changes (SEC, DLS) or in a concentration limited range (FRET) leading to arbitrary results. [1, 3, 4] Approaching this open question with analytical ultracentrifugation (AUC), we are able to distinguish three different oligomeric states. By comparing the oligomer distributions from AUC with forward scattering from small angle X-ray scattering (SAXS) experiments, we can assign a distribution of monomers and dimers in nucleotide free (NF) and GppNHp-bound conditions. In presence of GDP  $\text{AlF}_x$ , we observe an equilibrium between dimers and tetramers. The solution structure of the oligomers is investigated with ab initio and rigid body modelling strategies.

Significant mechanistical changes have been reported due to a post-translational modification of the protein which is called farnesylation, but previous studies have been confined to the non-modified protein. The farnesylated protein is capable of building polymers that can be observed by using absorption spectroscopy. [6] Forward scattering in our SAXS experiments implicates a completely monomeric distribution in nucleotide free solution whereas the non-farnesylated protein is in an equilibrium of monomers and dimers under same conditions. We will investigate the polymeric structure and the polymerization kinetics using kinetic SAXS and DLS experiments.

[1] B. Prakash, et al., Nature. 567-71 (2000) 403(6769)

[2] A. Roux, et al., Proc. Natl. Acad. Sci. U S A. 4141-4146 (2010) 107(9)

[3] T. Voepel, et al., Biochem. 4590-4600 (2014) 53

[4] A. Syguda, et al., FEBS J. 2544-2554 (2012) 279

[5] T. Voepel, et al., J. Mol. Biol. 63-70 (2010) 400

[6] C. Dovengerds, Dissertation RUB. (2013)

**Lisa K. Mahnke**

[lmahnke@ac.uni-kiel.de](mailto:lmahnke@ac.uni-kiel.de)

CAU Kiel, WG Prof. Dr. W. Bensch

**PhD Student**

Institute of Inorganic Chemistry

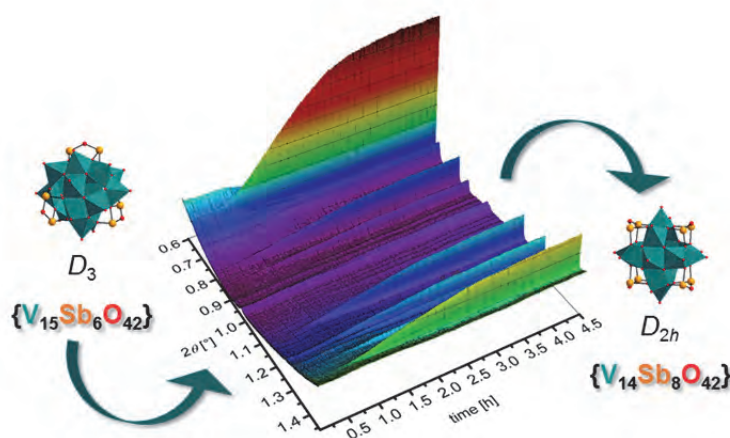
Max-Eyth-Strasse 2, 24118 Kiel, Germany

**Research interests:** Chemical Modification and Synthesis of Polyoxovanadates, *in-situ*-XRD Investigations



## Nucleation and Formation of a $\{V_{14}Sb_8O_{42}\}$ Cluster from a $\{V_{15}Sb_6O_{42}\}$ Hetero Polyoxovanadate: *In-Situ* XRD Studies

The chemical modification of polyoxovanadates is still a synthetic challenge. The compound  $\{Ni(en)_3\}_3[V_{15}Sb_6O_{42}(H_2O)] \cdot \approx 15H_2O$ <sup>[1]</sup> (compound **I**) represents the first water soluble hetero-polyoxovanadate which is a powerful synthon for the generation of new antimony-substituted polyoxovanadates crystallizing within extremely short reaction times compared to normally applied synthesis conditions. Under solvothermal conditions and stirring the aqueous solution compound **I** is *in-situ* transformed to  $\{[Ni(en)_2]_2V_{14}Sb_8O_{42}\} \cdot nH_2O$  (compound **II**). The chemical composition of **I** and **II** as well as the crystal structures suggest enormous changes occurring during the reaction. *In-situ*-XRD investigations were performed at the “Deutsche Elektronen Synchrotron in Hamburg, DESY”. The results were examined and evaluated with respect to the kinetics of crystal growth and nucleation.<sup>[2]</sup> The results demonstrate a very fast disappearance of crystalline **I**, an induction period depending on the reaction time and a very fast growth of the final product **II**. The transformation reaction is complete within a few hours. From temperature dependent *in-situ* XRD experiments very low activation energies for nucleation and crystal growth were obtained. Evaluation of the kinetics suggests that the nucleation process is autocatalytic. In the poster the results are presented and discussed.



[1] M. Wendt, U. Warzok, C. Näther, J. van Leusen, P. Kögerler, C. A. Schalley, W. Bensch, *Chem. Sci.* (2016) **7**, 2684-2694.

[2] M. Wendt, L. Mahnke, N. Heidenreich, W. Bensch, to be published.

## **Nikita Marchenkov**

Marchenkov\_nv@nrcki.ru

National research center «Kurchatov institute»

**Deputy director on scientific work**

**of NBICS-technologies Kurchatov complex**

1, Akademika Kurchatova pl., Moscow, 123182, Russia

**Research interests:** X-ray diffraction, defect structure, single crystal structure diagnostics, x-ray diffraction in crystals under external influence, piezoelectric properties of crystals



### **Development of X-Ray diffraction techniques for investigation of single crystals defect structure behavior under external electric field and piezoelectric properties characterization.**

The methods for measuring piezoelectric constants of crystals of different crystal systems by X-ray quasimultiwave diffraction and triple-crystal diffractometry are proposed and implemented. These techniques make it possible to determine the piezoelectric coefficient by measuring variations in the lattice parameter under an external electric field [1]. These methods have been approved, their potential is evaluated, and a comparison with high-resolution X-ray diffraction data is performed.

The formation of unusual slowly relaxing domains under an external dc electric field has been revealed in paratellurite ( $\text{TeO}_2$ ) crystals [2]. These domains differ from those arising in ferroics (ferromagnets, ferroelectrics, ferroelastics, etc.). The effect is characterized by the existence of a threshold field strength (at which domains begin to be formed) and long equilibrium settling times (up to a few hours, depending on the electric field strength). A crystal returns to the initial single-domain state also after a few hours after the field is switched off. High-resolution triple-crystal X-ray diffractometry has revealed that domains retaining the paraelastic tetragonal phase rotate with respect to each other in space without changing their lattice parameter. The domain sizes are 2-4  $\mu\text{m}$ , depending on the field strength. Currently, the exact mechanisms of domain formation are unclear. Possible reasons for the formation of these defects and an analogy of the observed effects with the behavior of liquid crystals under electric field are discussed.

This work was supported by *Grant RFBR № 16-32-60045 MOL\_A\_DK*.

[1] Blagov A.E., Marchenkov N.V., Pisarevsky Yu.V., et al., Cryst. Rep. 49-53 (2013) 58.

[2] M. V. Kovalchuk, A. E. Blagov, A. G. Kulikov, et al., Cryst. Rep. 862–866 (2014) 59.

## Margarita Marchenkova

[marchenkova@crys.ras.ru](mailto:marchenkova@crys.ras.ru)

Shubnikov Institute of Crystallography of Federal Scientific Research  
Centre “Crystallography and Photonics” of Russian Academy of  
Sciences

### Research scientist

59, Leninsky pr., Moscow, 119333, Russian Federation

[marchenkova\\_ma@nrcki.ru](mailto:marchenkova_ma@nrcki.ru)

National Research Centre “Kurchatov Institute”

### Research engineer

1, Akademika Kurchatova pl., Moscow, 123182, Russian Federation

**Research interests:** Interaction of X-rays and neutrons with matter,  
Langmuir monolayers, protein crystallization



## Creation of partially ordered organic planar systems based on *in situ* control of their structural organization

The possibility of quality improving of the planar systems based on photoactive porphyrin-fullerene dyads, cytochrome *c* and cardiolipin, lysozyme crystals and films by means of *in situ* X-ray techniques and molecular modeling complex is described. The proposed approach to control all stages of the creation of organic partially ordered structures is shown to be effective during the *in situ*-study from the complexes formation in solutions to the growth of protein crystals and films.

Based on this approach, the structure of Langmuir monolayers of photoactive porphyrin-fullerene dyads both on the air-water interface and on the solid substrate has been studied using X-ray methods (X-ray reflectometry and X-ray Standing Wave technique (XSW) at the Total Reflection Condition) [1]. The kinetics of cytochrome *c* with cardiolipin Langmuir monolayer interaction was investigated [2]. A technique for the *in situ* study of the growth of protein crystals and ordered systems on substrates is described. The self-organization of protein molecules in the solution, as well as protein molecules state change at an early stage of crystallization is examined for tetragonal lysozyme. On the base of analysis of the crystal structure of the lysozyme, the different oligomers were simulated, which may be the elementary units of the crystal growth [3].

[1] Y.A. Dyakova, et al., Mendeleev Commun. 149-151 (2016) 26

[2] M.A. Marchenkova, et al., Langmuir. 12426 (2015) 31

[3] M.V. Kovalchuk, et al., Cryst. Growth Des. 1792 (2016) 6

## **Leonid Mazaletskiy**

[boolvinkl@yandex.ru](mailto:boolvinkl@yandex.ru)

P.G. Demidov Yaroslavl State University

**PhD student**

Russia, Yaroslavl, Sovetskaya st., 14

**Research interests:** Nanotechnology, Composite materials, Scanning electron microscopy



### **Influence of porosity on charge-discharge characteristics of silicon-based thin-filmed negative electrode in lithium-ion batteries**

The results of experimental studies of porous silicon nanocomposite materials for future usage as an anode material of lithium-ion batteries are presented. Nowadays batteries, based on lithium-ion technology, come more and more popular. This is because this type of batteries is lighter, powerful, and has smaller dimensions than batteries based on other technologies. In this paper we propose to use well-known silicon as active material for anodes of lithium-ion batteries. Its big advantage is charge capacity – 4211 mAh/g [1,2]. But key disadvantage that stops wide usage of silicon for anodes is that the introduction of 4 lithium atoms per one silicon atom leads to rapid destruction of the silicon. That's why we have to make anode material composite - include oxygen and aluminum to its compound.

Also for acceleration of lithium intercalation process the structure of nanocomposite material should be porous. After this it will be easier for lithium ions to penetrate with structure, and charge-discharge process will go faster. This investigation is aimed to improve charge-discharge characteristics. Comparison between original and porous structures in terms of their qualitative and quantitative characteristics is given. Received data tells that with porous structure in nanocomposite anode material samples can handle bigger currents and not collapse. This will let to create more powerful lithium-ion batteries in future.

This work was carried out at the equipment of the Facilities sharing centre “Diagnostics of Micro- and Nanostructures” and was supported by the Ministry of Education and Science of the Russian Federation (project no. 14.574.21.0099; unique project ID RFMEFI57414X0099).

[1] R.A. Sharma, R.N. Seefurth, J. Electrochem. Soc. 1763–1768 (1976) 123

[2] C.J. Wen, R.A. Huggins, J. Solid State Chem. 271-278 (1981) 37

## **Svetlana Medvedeva**

[smedvedeva@innopark.kantiana.ru](mailto:smedvedeva@innopark.kantiana.ru)  
Immanuel Kant Baltic Federal University

**Junior researcher**

Nevskogo, 14, Kaliningrad 236000 Russia

**Research interests:** Investigation of micro- and nanostructures by X-ray microscopy, diffraction and reflectometry



### **Creation of Al/Ni based multilayer structures by Ion-Beam Deposition method for experimental applications at synchrotron radiation sources.**

Recently Multilayer Structures (MS) have found a very wide range of applications: from X-ray optic elements [1-2] and special structures for X-ray standing waves generators [3], to laser mirrors, neutron optics and telescope components. Few nanometers (1-10 nm) of individual uniform layer thickness, angstrom-smooth interfaces and number layers up to several hundred are standard requirements for modern multilayers.

In this work, we report growth and application of thin film structures, fabricated by Ion-Beam Deposition method. This technique is an ideal tool for large area deposition and allows a wide range of working materials. Particularly it can produce Kr-plasma instead Ar-plasma. High sample quality without thickness gradient was achieved by using rotating target system to deposit all layers in one vacuum process.

The grown MS consisted of twenty pairs of alternating Al/Ni layers with the thickness of 3 nm per each layer. The first type of MS were deposited in Ar plasma, the second type – in Kr plasma. The multilayers were studied by atomic force microscopy and X-ray reflectivity technique. Finally, experiments were carried out using these MS as X-ray standing waves generators at the PETRA III synchrotron in Hamburg.

Surface profile demonstrates low surface roughness not exceeding 0.4 nm. High reflectivity value of the first Bragg peak is approximately 50 % at 8.048 keV, which is very near to the theoretical value. This demonstrates a high degree of MS period uniformity.

[1] F. Doring, et al., Optics Express, Vol. 21, No. 16 (2013)

[2] X. Huang, et al., Optics Express, Vol. 23, No. 10 (2015)

[3] E. Schneck, et al., Current Opinion in Colloid & Interface Science Vol. 20 244-252 (2015)

## **Masoud Mehrjoo**

[Masoud.mehrjoo@xfel.eu](mailto:Masoud.mehrjoo@xfel.eu)

1 - University of Hamburg, The Hamburg Centre for Ultrafast Imaging

2 - European XFEL GmbH

### **PhD Student**

1 - Luruper Hauptstraße 149, 22547 Hamburg, Germany

2 - European XFEL GmbH ,Holzkoppel 4,  
22869 Schenefeld , Germany

**Research interests:** Coherent diffractive imaging, X-ray Correlation Spectroscopy, Dynamics of Complex systems



## **Towards Single-Shot Measurements of Focused FEL Wavefronts using Iterative Phase Retrieval**

The advent of Free-Electron-Lasers (FELs) enables new insight into many fields of science. These new sources provide ultra short, high peak brilliance and coherent pulses, offering numerous scientific opportunities ranging from observing optical nonlinear effects, to study matter in extreme conditions.

At currently operating FEL sources, the pulsed radiation produced primarily relies on the stochastic process of Self-Amplitude Spontaneous Emission (SASE), originating from random fluctuations in the driving electron bunches. Thus the complex wavefronts can fluctuate dramatically from shot-to-shot and possess stochastic features in every single shot.

Intuitively, a detailed understanding of FEL based experiments requires potentially prior knowledge of the spatial distribution of each complex wavefront<sup>1</sup>. We report on a high resolution coherent imaging technique, based on the modified near field phase retrieval algorithm<sup>2</sup>, to fully characterize single-shot highly focused FEL pulses<sup>3</sup>.

Exploiting the strong curvature of a divergent beam downstream of the focal plane, ensures the uniqueness of the iterative solution and reliable, fast convergence<sup>4</sup>. This method can be compared with Hartman Wave Front Sensing (HWS), a well-established, but relatively low-resolution method for characterizing long wavelength FEL beams<sup>5</sup>.

We show complex wavefront reconstructions for many individual pulses collected at a variety of different source parameters. The difference between individual pulses for the same source parameters, as well as the difference between sets of pulses for different source parameters are explored. This statistical overview can help to potentially connect the reconstructed wavefronts to the relevant ideal source parameters, as well as exploring the natural variations of FEL wavefronts for different source parameters.

1. A. Schropp et al., Scientific Reports 3, 1-5 (2013).
2. J. R. Fienup, Applied Optics 21, 2758-2769 (1982)
3. H. M. Quiney et al., Nature Physics 2, 101-104 (2006).
4. K. A. Nugent et al., Acta Cryst. 61, 373-381(2005).
5. B. Floter et al., New Journal of Physics 12, 1367-1382 (2010).

**Irina Miloichikova**

[miloichikova@gmail.com](mailto:miloichikova@gmail.com)

National Research Tomsk Polytechnic University

**PhD student**

634050, Tomsk, Lenin Avenue, 30

**Research interests:** Medical physics, Clinical dosimetry, Tomography



## **The analysis of the X-ray and synchrotron radiation suitability for the subcellular investigation of the flaws in wood**

Nowadays, for ecological monitoring high attention is paid to biological indication techniques, which allows to estimate integrated effect of pollutants on living organisms. As bioindicators of atmosphere pollution is widely used woody plants. Coniferous species having a low, in comparison with deciduous trees, metabolic rate, perennial assimilative organs, imperfect conductive system, are the most sensitive to contamination. The main structural changes affect sprout wood and needle [1-3].

A number of studies show that the Siberian cedar demonstrates specific changes under influence of industrial pollution. Analysis of the needle anatomical sign identifies that for this species of wood under technogenic stress conditions the area of mesophyll, central cylinder, vein and resin channels are decreased [4]. Standard methods of the sprout wood and needle anatomical research, based on optical microscopy, have following disadvantages: flares are appeared on the image for high magnification, which prohibited to carry out investigations with desired precision.

An alternative method of data acquisition can be X-ray imaging of biological cells [5]. For the purposes of obtaining more sharply image of the sprout wood and needle cross sections it was proposed to use a method based on X-ray projections receiving on LiF detectors using polycapillary optics, this method is described more specifically in [6].

Another solution could be using of synchrotron X-ray microscopy methods, which have a number of advantages, such as higher contrast and spatial resolution and lesser radiation damage of the sample. The sprout wood and needle anatomical research can be realize at the station "Tomography and Microscopy" on the synchrotron radiation channel of the VEPP-3 accelerator complex of Budker Institute of Nuclear Physics (Novosibirsk) [7].

It is expected that the data obtained by X-ray and synchrotron radiation allows us to investigate the sprouts wood and needles cellular structure more accurately, which in turn will increase the ecological monitoring effectiveness based on plants condition research.

[1] Ganon J.A., Qiu H.L. Ecological Application of Remote Sensing at Multiple Scale // Handbook of Functional Plant Ecology // Ed. by F.I. Pugnaire, F. Valladores N.Y.: Marcel Dekker, 1999

[2] A.N.D. Auclair, et al., Water, Air, and Soil Pollution 13-31 (1990) 53

[3] H.K. Lichtenthaler, J. Plant Physiol. 4-14 (1996) 148

[4] A.P. Zotikova, et al., Tomsk State University J. 197-200 (2007) 299 [in Russian]

[5] C.Y.J.Hémonnot, et al., ACS nano 3553-3561 (2016) 10.3

[6] D. Hampai, et al., EPL 60010 (2011) 96

[7] K.E. Kuper, et al., Nucl. Instrum. Methods Phys. Res., Sect. A 255-258 (2007) 575.1

## **Tatiana Mishurova**

[tatiana.mishurova@bam.de](mailto:tatiana.mishurova@bam.de)

Federal Institute of Materials Research and Testing (BAM)

**PhD student**

Unter den Eichen 87, 12205, Berlin, Germany

**Research interests:** Micro-computed tomography, neutron diffraction, synchrotron x-ray diffraction, residual stresses, material science, metal matrix composites



### **The role of reinforcement orientation on the damage evolution of short-fibre reinforced metal matrix composite under compression**

In the present study, internal damage to an AlSi12CuMgNi alloy reinforced with planar random Al<sub>2</sub>O<sub>3</sub> short fibres was investigated after compression testing. Due to the alloy composition, this composite contains a second reinforcement phase in the form of eutectic Si, which builds interpenetrated networks in the volume and increases the creep resistance and load-bearing capacity of the material [1]. Materials with their fibre plane parallel and transversal to the load direction were characterized in order to investigate the dependence of load partition and damage on fibre plane orientation. *In-situ* compression testing during neutron diffraction measurements showed that internal damage is strongly influenced by the load partition between matrix and reinforcement. Moreover, micro-computed tomography was performed in the same material after *ex-situ* compression for damage analysis. In the case of a fibre plane perpendicular to the applied load, breakage and interconnected cracks appeared in a significantly higher volume fraction than with a fibre plane parallel to load [2].

[1] G. Requena, P. Degischer, E. Marks, E. Boller, *Mat Sci and Eng A*, 487 (2008) 99–107.

[2] S. Cabeza, T. Mishurova, G. Bruno, G. Garcés, G. Requena, *Scripta Mat.*, 112, (2016) 115–118.

[2]. S. Cabeza, T. Mishurova, G. Bruno, G. Garcés, G. Requena, *Scripta Mat.*, 112, (2016) 115–118.

## Alexander Mistonov

[mistonov@lns.pnpi.spb.ru](mailto:mistonov@lns.pnpi.spb.ru)

Saint Petersburg State University

Senior lecturer

Russia, Saint Petersburg, Peterhof, Ulyanovskaya, 1

**Research interests:** Condensed matter physics, magnetism, spin ice



### Interplay between of “ice-rule” and external magnetic field in inverse opal-like structures

We study magnetic properties of inverse opal-like structure (IOLS) based on Co. It was prepared by templating technique: the voids of face-centered-cubic (fcc) opal, which was constructed of 590 nm microspheres, were filled with Co by an electrochemical crystallization. Then, the microspheres were dissolved in toluene and free-standing ferromagnet net was obtained. The IOLS is built of unit elements, consisting of three parts: two quasitetrahedra and one quasicube with concave faces. These parts are connected by vertices along  $\langle 111 \rangle$  directions of fcc structure.

The IOLS are interesting as a 3D nanoscale analogue of spin-ice. In analogy to the “spin ice rule”, the magnetic flux conservation law for the elements of the IOLS must be fulfilled. Previously, on this basis we have developed a model for the distribution of magnetization vectors along  $\langle 111 \rangle$  axes within the IOLS.

In this work we have performed neutron small angle diffraction experiment in attempt to verify the model. During the experiment external magnetic field was directed along  $[111]$ ,  $[100]$  and  $[1-21]$  axes. Magnetic scattering intensities as a function of the field for the Bragg peaks of 202-family have been obtained. A difference between the curves for these geometries can be explained, in terms of different scenarios of the interplay between of the “ice-rule” and the field. In the first one, the field competes to the “ice-rule”, and the situation (3-in-1-out) arises, when the magnetic field breaks the ice-rule. In the second geometry the “ice-rule” and magnetic field interfere constructively, because the “ice-rule” is fulfilled, when all vectors have positive projections on the field direction, thus minimizing the Zeeman energy. In the third geometry, when one vertex is perpendicular to the field (i.e. does not depend on it), possible magnetic configurations in the IOLS are determined by the “ice-rule”.

**Dmitrii Nesterov**

[nesterov@phys.vsu.ru](mailto:nesterov@phys.vsu.ru)

Voronezh State University

**Researcher**

Universitetskaya pl. 1, 394018, Voronezh, Russia

**Research interests:** X-Ray and electron spectroscopy and microscopy,  
electronic structure of silicon based structures, nanosystems,  
synchrotron studies of functional materials



## 2D and 1D silicon materials electronic structure by synchrotron studies

As 2D silicon based nanosystem the electronic structure of SOI (silicon-on-insulator) with strained and unstrained silicon layers was theoretically calculated and experimentally investigated by means of Ultrasoft X-ray Emission and Absorption Spectroscopy. According to the experimental results, an additional spectral feature occurs in the strained silicon layer density of states near the bottom of the conduction band ( $E_c$ ). The shift of  $E_c$  towards the top of the valence band, as well as smoothing of the density of states and disappearance of the degenerate minimum between  $L'_{2v}$  and  $L_{1v}$  valence band states was also observed. For the first time Synchrotron Radiation (SR) interference phenomena is observed for the strained silicon nanolayer applied to dielectric  $\text{SiO}_2$  layer on Si (100) single crystalline substrates (SOI structures). Strong oscillation of spectra intensity in dependence on photon energy is detected in energy range before elementary silicon Si  $L_{2,3}$  absorption edge ( $\leq 100$  eV) with SR grazing angles lower than  $21^\circ$  in X-ray photoeffect quantum yield structure. Phase of the spectra oscillation structure is reversed with small variations of grazing angles in  $4^\circ$ – $21^\circ$  range. The theoretical calculations have been performed by full potential linearized augmented plane-wave method and it was shown that straining of silicon lattice leads to a slight shifting of the conduction band bottom towards the top of the valence band and causes an increase in the density of states between  $L'_{2v}$  and  $L_{1v}$ . The theoretical shift of the conduction band bottom is substantially less than the experimental one.

Silicon nanowires massives were studied as 1D silicon based nanosystem. Essential differences in electronic structure and phase composition of silicon nanowires were demonstrated by X-ray spectroscopy techniques. Massives of the ordered silicon nanowires have been produced by metal assisted wet chemical etching of the crystalline silicon substrates. The formed massives and individual nanowires have been studied by scanning and transmission electron microscopy. Electronic structure and phase composition studies of the surface and near surface layers of the massives were performed by laboratory based Ultrasoft X-ray Emission Spectroscopy and synchrotron based X-ray Absorption Near Edge Structure Spectroscopy. It is shown that the sample that are morphologically more developed and formed on a substrate with low resistivity is considerably more strongly subjected to oxidation with noticeable formation of intermediate silicon oxides phases. The massive of nanowires formed on a substrate with high resistivity also naturally oxidized, but to a lesser extent and contained the phase of crystalline silicon with the increase of the probation depth. The anomalous effect of the synchrotron radiation interaction with the silicon wires structure formed at the low doped substrate is detected as the inversed intensity effects. The explanation model for the observed peculiarity is suggested.

The authors acknowledge the support by the Ministry of Education and Science of Russia in frameworks of state task for higher education organizations in science for 2014-2016: Projects 757, 1606 and N 3.1868.2014/K. We thank HZB for the allocation of synchrotron radiation beamtime.

## **Evelina Nikelshparg**

[evelinanick@gmail.com](mailto:evelinanick@gmail.com)

Department of Biophysics, Biological Faculty, Moscow State University

**PhD student**

Leninskie gory 1/12, Moscow, Russia

**Research interests:** Surface-enhanced Raman spectroscopy (SERS), mitochondria, cytochromes



### **SERS-based approaches to study biomolecules and living organelles**

Surface-enhanced Raman spectroscopy (SERS) is a powerful tool to investigate conformation of different molecules in intact state. It is based on a great enhancement of Raman signal from molecules in a close vicinity to nanostructures with plasmonic properties. Heme molecules are likely to be investigated by means of Raman spectroscopy because they have intensive Raman spectra allowing to determine the conformation and redox state of a heme and spin state of heme iron. However study of hemes inside living cells and organelles is hardly achievable because of complex composition of hemes and low signal intensity of conventional Raman spectroscopy. SERS is used to enhance Raman signal from molecules significantly which makes it a promising tool for heme investigation *in situ*. Previously it was demonstrated that SERS can be applied to probe submembrane hemoglobin in living erythrocytes [1]. Recently we proposed a novel label-free SERS-based approach to study cytochromes in living mitochondria [2]. Mitochondria are organelles in eukaryotic cells which provide energy supply, participate in carbohydrate and lipid metabolism, signaling and apoptosis regulation. There are various types of cytochromes in mitochondria which are difficult to distinguish using spectroscopic tools. SERS of mitochondria placed on silver plasmonic nanostructures under green laser irradiation was shown to be able to probe cytochrome *c* separately from other cytochromes and to investigate its redox state and conformation of porphyrin. We showed that SERS spectra of cytochrome *c* were sensitive to the activity of mitochondrial respiration and inner membrane potential. Furthermore, we proposed a number of silver-based nanostructures of different morphology with plasmon resonance bands in visible region to investigate living cells and organelles using SERS [3].

[1] N.A. Brazhe, et al., *Biophys J.* 3206–3214 (2009) 97(12)

[2] N.A. Brazhe, et al., *Sci Rep.* 13793 (2015) 5

[3] A.S. Sarycheva, et al., *J. Mater. Chem. B.* 539-546 (2016) 4

## Fan Pan

[fanpan@kth.se](mailto:fanpan@kth.se)

Department of Materials and Nano Physics, School of Information and  
Communication Technology, KTH Royal Institute of Technology

### PhD student

KTH Royal Institute of Technology, Electrum 229, SE-16440 Kista,  
Sweden

**Research interests:** Finite temperature Magnetism, Atomic spin  
dynamics, Gilbert damping



### **A systematic study of magnetodynamic properties at finite temperatures in doped permalloy from first principles calculations**

By means of first principles calculations, we have systematically investigated how the magneto-dynamic properties Gilbert damping, magnetization and exchange stiffness are affected when permalloy (Py) ( $\text{Fe}_{0.19}\text{Ni}_{0.81}$ ) is doped with 4d or 5d transition metal impurities. We find that the trends in the Gilbert damping can be understood from relatively few basic parameters such as the density of states at the Fermi level, the spin-orbit coupling and the impurity concentration. The temperature dependence of the Gilbert damping is found to be very weak which we relate to the lack of intra-band transitions in alloys. Doping with 4d elements has no major impact on the studied Gilbert damping, apart from diluting the host. However, the 5d elements have a profound effect on the damping and allows it to be tuned over a large interval while maintaining the magnetization and exchange stiffness. As regards spin stiffness, doping with early transition metals results in considerable softening, whereas late transition metals have a minor impact. Our result agree well with earlier calculations where available. In comparison to experiments, the computed Gilbert damping appears slightly underestimated while the spin stiffness show good general agreement.

[1] arXiv 1602.06201 Fan Pan *et al*, (2016)

**Elena Parinova**

[parinova@phys.vsu.ru](mailto:parinova@phys.vsu.ru)

Voronezh State University

**Researcher at the solid state physics and nanostructures department**

394018, Russia, Voronezh, Universitetskaya pl., 1

**Research interests:** X-ray and electron spectroscopy and microscopy, electronic structure of silicon based structures, nanosystems, synchrotron studies of functional materials



### **Application of the photoemission electron microscopy for the precision nanostructures diagnostics with the use of the synchrotron radiation**

The precision characterization of nanostructures and reconstruction of their atomic and electronic structure requires a complex of suitable experimental methods including ones achievable with the use of the small spot spectroscopy. Small spot characterization in its turn necessitates the microscopy approach e.g. for the possibility of finding the surface area under study of the whole structure. Moreover examination of the surface morphology for the objects under investigation is a crucial point for nearly every study. In turn, X-ray and electron spectroscopy are traditionally used to obtain information about the physical-chemical nature of the objects. These methods are nondestructive and highly sensitive to properties of thin (from a few nanometers to a few tens of nanometers) subsurface layers, which makes them particularly important for analysis of novel materials and functional structures. Such methods as photoelectron spectroscopy and X-ray absorption spectroscopy are highly sensitive to the local surrounding of atoms of a particular type (especially in the case of synchrotron radiation used for excitation of the spectrum) and provide information about specific features of the atomic and electronic structure of the studied object.

Information obtained by photoemission electron microscopy (PEEM) combines the microscopic component, which gives an insight into the surface morphology of the object under study, and the spectroscopic component, which makes it possible to obtain the X-ray spectrum of the chosen microscopic field of view fragments. The use of the synchrotron radiation allows to obtain the terminal lateral and energy resolution because of its unique properties such as naturally high collimation, photon intensity, polarization possibilities, etc.

Our work presents results of the investigation of magnetic submicron nickel rods arrays in the SiO<sub>2</sub> matrix by means of the PEEM method in X-ray absorption near edge structure (XANES) registration mode with high intensity synchrotron (undulator) radiation. We have demonstrated the efficiency of using PEEM technique. It has been shown that rod-like structures and bridges between them are formed of a bulk nickel phase, which is stable to natural oxidation. Apparently, this is associated both with a dense microstructure of the precipitate (the absence of micro- and nanopores in the metal) and with the encapsulation of this precipitate by chemically stable silica. It has been found that no formation of intermediate compound phases (nickel silicides and oxides) is microscopically observed at the Ni/SiO<sub>2</sub> heterojunction, whereas oxidized nickel(II) species are identified on the surface of the SiO<sub>2</sub> matrix in nearly noticeable amount. Surface remanent magnetization are patterned at the room temperature with and without the applied magnetic field that is shown at microscopic level as well by PEEM. With this example we have demonstrated the excellent combination of microscopy and spectroscopy approaches at one spot aiming the precision, clear and deep novel materials characterization. This technique can be used for a wide range of modern diagnostics tasks up to biology and cultural heritage applications.

The authors acknowledge the support by the Ministry of Education and Science of Russia in frameworks of state task for higher education organizations in science for 2014-2016: Projects 757, 1606 and N 3.1868.2014/K. We thank HZB for the allocation of synchrotron radiation beamtime.

## **Ilia Petrov**

[ia.petrov@physics.msu.ru](mailto:ia.petrov@physics.msu.ru)

Faculty of Physics, M.V. Lomonosov Moscow State University

### **Master Student**

Faculty of Physics, M.V. Lomonosov Moscow State University,  
Leninskie Gory, Moscow 119991, Russia

X-ray free-electron lasers

**Research interests:** Diffraction of ultrashort femtosecond impulses in multilayer structures with lattice distortion



## **Analysis of the formation of delayed X-ray pulses in multilayer structures**

At XFELs (x-ray free-electron lasers), the application of delayed ultrashort femtosecond and sub-femtosecond pulses is of great interest, for instance, for pump-and-probe experiments and self-seeding. Theoretical investigation of the formation of delayed ultrashort x-ray pulses in multilayer structures has been performed. Small distortions of lattice in various layers allow to obtain time delay in both cases of reflection and transmission. Temporal structure and intensity of delayed pulses have been observed in dependence on various parameters of the structure, such as thickness, number of periods and lattice distortions. Low mass absorption materials are preferred for the needs of formation of delayed pulses. Methods of practical application of the investigated structures have been proposed alongside with requirements to the parameters of the delay line. Efficiency and drawbacks of the methods are discussed. Prospect of development of the method is provided.

[1] V.A. Bushuev, I.A. Petrov. Analysis of the formation of delayed X-ray pulses in multilayer structures. Abstract book of «X-ray Optics - 2016» conference, 26-29 September 2016, Chernogolovka, Russia.

## **Petai Pip**

[petai.pip@lbf.fraunhofer.de](mailto:petai.pip@lbf.fraunhofer.de)

**Master student**

Fraunhofer LBF Darmstadt, Germany

Technical University Darmstadt, Germany

**Research interests:** Polymers, Morphology and Dynamics, Fracture Mechanics



### **Molecular understanding of fracture mechanisms of semi-crystalline polymers**

Although semi-crystalline polymers so as polyolefinic materials are widely used, a complete molecular picture about the underlying mechanisms of fracture is still missing. The structure of semi-crystalline polymers ranges from the atomic length scale of the crystal cell up to spherulithic or other superstructures on the submillimeter scale.

The hierarchical structure is generated by molecular motions of the macromolecules during crystallisation from the melt. Fracture mechanics is related to molecular rearrangements in short as well as long-time scales such as ductile fracture, slow creep and slow crack growth: These mechanisms are far from linear (viscoelastic) behaviour. Continuum concepts of fracture mechanics are the stress intensity factor, crack tip opening displacement (CTOD) or the J-integrale. On the other hand, there are molecular failure mechanisms such as disentanglement, chain breakage or cavitation. A molecular understanding requires a broad spectrum of experimental methods (see e.g. [1]) to discover both, structural changes and molecular relaxations. The knowledge of the underlying mechanisms is of practical importance for the durability of pipes or blow molded containers for hazardous material of dangerous goods but also for most other high-performance applications.

The focus of this work is related to the understanding of molecular processes and structural changes in semi-crystalline polymers during mechanical load. For detection of those morphological changes scattering experiments by small-angle and wide-angle X-ray scattering imaging methods are well established. In order to detect the orientation of the semi-crystalline structure under load prior fracture we developed an ultrasonic setup to measure ultrasonic velocity and attenuation under load. Therefore, we combine a pulse-transition technique with a tensile test setup. The orientation of the crystalline structure is expected to be reflected by an increase of the sound velocity and the related longitudinal modulus [2].

For this study, we selected high density polyethylen (PE-HD) of different molecular structure such as different molar mass distribution (monomodal, di- and trimodal) as well as different copolymer content and distribution. The samples were characterized by gel permeation chromatography (GPC), tensile testing, fracture tests, dynamic mechanical and thermal analysis, infrared and NMR spectroscopy.

[1] T. Kida, Y. Hiejima, K.H. Nitta, *eXPRESS Polymer Letters* 10 (2016) 701

[2] G. Perez, in *High speed fiber spinning*, Ed. by A. Ziabicki and H. Kawai, John Wiley & Sons, Inc. 1985, ch. 12, p. 333-362

## Mikhail Platonov

[ms-platonov@yandex.ru](mailto:ms-platonov@yandex.ru)

Kirensky Institute of Physics

Researcher

Akademgorodok 50/38, Krasnoyarsk, 660036 Russia

**Research interests:** Magnetic materials, Interplay between structure and magnetism, XAFS and XMCD



### **Crystal and local atomic structure of $\text{MgFeBO}_4$ , $\text{Mg}_{0.5}\text{Co}_{0.5}\text{FeBO}_4$ , and $\text{CoFeBO}_4$ : Effects of Co substitution**

In the present work, a careful study of the electronic state, long-range, and local structural properties of three-component warwickite system  $\text{Mg}_{1-x}\text{Co}_x\text{FeBO}_4$  has been carried out. XANES/EXAFS spectra analysis [1] is supported by X-ray crystallographic data to build up a wide view of the electronic state and local structure of metal ions.

The X-ray diffraction and XANES analysis in this work have shown unambiguously that Mg and Co enter in the warwickite structure in divalent state, while Fe enters in the trivalent state. Those experiments also show the existence of some preferential occupation habits of  $\text{Fe}^{3+}$ . In fact, the information on the occupation probabilities of the two sites can be complemented by the partial information on their occupation by the Fe atoms, provided by Mössbauer spectroscopy (MS) [2]. In  $\text{MgFeBO}_4$  there is qualitative agreement, since both techniques indicate that  $\text{Fe}^{3+}$  enters mostly at the M1 site, while in  $\text{CoFeBO}_4$  MS spectra analysis shows that  $\text{Fe}^{3+}$  sits with a larger probability at the M2 sites. Low-symmetric Jahn-Teller-like distortions exist for both coordinated octahedra as can be seen from the normal coordinates calculations. As the Co content increases, the structural distortions become more pronounced. An alternation of the octahedra principal axes within the ribbon was found.

The XRD data yield the average M - O distances over the two metal Fe and Co, so the increasing distortion cannot be assigned either to Fe or Co atoms. In spite of this,  $V_{zz}$  calculated with those data increases with Co content and shows that Co atoms plays an important role in the structure modification. The effect of Co substitution is clarified by means of the element selective techniques XANES and EXAFS data. The average interatomic distances Fe - O and Co - O provide direct evidence for trivalent and divalent states of iron and cobalt ions, respectively. The electronic states of the Fe and Co are not affected by the substitution. The substituted Co ions have two roles: one is pushing the Fe atom from M1 site to M2 site, which is expressed in the reduction of the M2 site volume, and the other is an increase in the local distortions in  $\text{FeO}_6$  and  $\text{CoO}_6$  octahedra. In addition to XRD data, EXAFS analysis revealed that the Fe-O short bonds are smaller than the Co-O ones. So, the tetragonal distortions are expected to be greater for  $\text{FeO}_6$  octahedra than for  $\text{CoO}_6$  ones. At the same time the substitution of  $\text{Fe}^{3+}$  ions by  $\text{Co}^{2+}$  ions at the M1 site induces an increase in the rhombic distortion of  $\text{M1O}_6$  octahedra.

Finally, we may infer that the local structure distortions around the magnetic Fe and Co atoms play an important role in magnetic properties [3] and in magnetic crystalline anisotropy, especially.

This study was supported in part by the grants of the Council for Grants of the President of the Russian Federation (SP-938.2015.5, NSh-7559.2016.2), the Russian Foundation for Basic Research (project nos. 16-32-60049 mol\_a\_dk, 16-32-00206 mol\_a), the grant of Krasnoyarsk Region Science and Technology Support Fund and by the UMNIC program. The author is grateful to the Organizing Committee (NRC «Kurchatov Institute») the possibility to participate in a scientific school and for the financial support.

[1] Kazak N. V., et al., Phys. Status Solidi B 252.10 (2015) 2245-2258.

[2] Lyubutin I.S., et al., J. Alloys and Comp. 642 (2015) 204-209.

[3] Arauzo A., et al., JMMM 392 (2015) 114-125.

## Igor Plokhikh

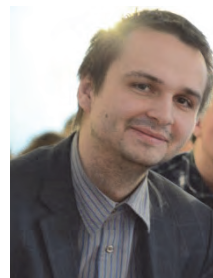
[ig.plohih@yandex.ru](mailto:ig.plohih@yandex.ru)

Lomonosov Moscow State University

Student

1 building 3 Leninskie Gory, 119991 Moscow, Russia

**Research interests:** inorganic chemistry, crystallography, X-ray diffraction, lanthanides



### **Novel layered compounds EuFZnPn and EuFMnPn (Pn = P, As, Sb) – synthesis, crystal structure and physical properties**

The investigation is devoted to new representatives of the LaOAgS structure type, interest to which grew in the last decade especially due to the discovery of superconductivity in iron arsenides, but also due to numerous peculiar physical properties like thermoelectricity, CMR effect, semiconductivity and some other, demonstrated by its representatives. This structure consists of alternating layers built by motifs of fluorite and anti-fluorite. It was recently shown [1] that new representatives can be designed by substituting  $[\text{Ln}_2\text{O}_2]^{2+}$  fluorite layers by isostructural layers with the composition  $[\text{Ae}_2\text{F}_2]^{2+}$ , where Ae is not only alkaline earth metals, but also  $\text{Eu}^{2+}$  owing to comparable with Sr radius of the latter. It is worth mentioning that each  $\text{Eu}^{2+}$  cation contains *seven* unpaired electrons and tends to form magnetically ordered states in solid compounds. Motivated by this we successfully synthesized *five* novel compounds.

In the series EuFMnPn we observe compounds for Pn = P, As, Sb, while in the series EuFZnPn the compound with Pn = P is absent. This fact we rationalized by calculating free enthalpy of the following reactions:  $\text{EuF}_2 + \text{EuZn}_2\text{Pn}_2 = 2\text{EuFZnPn}$ . For all new compounds we refined crystal structures using powder XRD data. The structures, including cell parameters and interatomic distances, appeared to be very close to known compounds from the series SrFZnPn and SrFMnPn [2]. For new compounds we made both magnetic susceptibility and heat capacity measurements, which reveal antiferromagnetic ordering in Eu sublattice in compounds EuFZnPn and EuFMnPn (Pn = As, Sb), and additional ordering in Mn-sublattice of manganese compounds. Noteworthy that EuFMnP is purely paramagnetic compound. Resistivity measurements and quantum calculations show that our compounds are narrow-band semiconductors. All results will be discussed more thoroughly in the report.

This work was supported by the grant № 16-03-00661A of the RFBR.

[1] H. Kabbour, et al., J. Mater. Chem. 3525-3531 (2005) 15(34)

[2] D. O. Charkin, et al., J. Alloys Compd. 644-649 (2014) 585

## Philipp Polzin

ppolzin@ac.uni-kiel.de

Christian-Albrechts-Universität of Kiel

Master student

Institute of Inorganic Chemistry Max-Eyth-Str. 2 24118 Kiel, Germany

Research interests: Polyoxovanadate, In-situ XRD, Solvothermal synthesis



### Synthesis of the new $[\text{Ni}(\text{phen})_3]_2\{[\text{Ni}(\text{en})_2]\text{V}_{15}\text{Sb}_6\text{O}_{42}\} \cdot 20 \text{H}_2\text{O}$ Polyoxovanadate through a cation exchange reaction

Philipp Polzin, Michael Wendt, Huayna Terraschke, Wolfgang Bensch\*

Institute of Inorganic Chemistry, Christian-Albrechts-Universität of Kiel, Max-Eyth-Str. 2,  
24118 Kiel, Germany. E-mail: wbensch@ac.uni-kiel.de.

Polyoxovanadates (POVs) are remarkable materials formed by well-defined building blocks, such as square-pyramids, octahedrons or tetrahedrons, leading to wide coordination geometry. The POVs are formed through self-assembled condensation reactions under solvothermal conditions and these functional materials show impressive chemical and physical properties, presenting therefore possible applicability in the industry e.g. as catalysts. Through the combination of POVs with lanthanide (Ln) ions or complexes, interesting luminescence properties could be expected. The synthesis of POVs with covalently attached lanthanide species would be a remarkable approach to obtain new types of magnetic-luminescent materials.<sup>[1]</sup> Here, the aim was to synthesize Ln-doped POVs. Therefore,  $\{\text{Ni}(\text{en})_3\}_3[\text{V}_{15}\text{Sb}_6\text{O}_{42}(\text{H}_2\text{O})] \cdot \approx 15\text{H}_2\text{O}$  cluster<sup>[2]</sup> (en = ethylenediamine) was reacted with an  $[\text{Eu}(\text{phen})_2(\text{NO}_3)_3]$  complex (phen = 1,10-phenanthroline) under solvothermal conditions. It was expected that the POV cluster exchanges the coordinated Ni complexes with the Eu complexes. Astonishingly, the  $[\text{Eu}(\text{phen})_2(\text{NO}_3)_3]$  complex was not integrated in the new compound, instead two additional  $[\text{Ni}(\text{phen})_3]^{2+}$  complexes were formed and the new  $[\text{Ni}(\text{phen})_3]_2\{[\text{Ni}(\text{en})_2]\text{V}_{15}\text{Sb}_6\text{O}_{42}\} \cdot 20 \text{H}_2\text{O}$  (Fig. 1) was obtained. Moreover, the crystal structure of this new compound reveals a fascinating reorganization of one left  $[\text{Ni}(\text{en})_3]^{2+}$  complex to form a bridging  $[\text{Ni}(\text{en})_2]^{2+}$  complex, connecting two POV-clusters to a 1D chain structure. Further investigations, for example, *in-situ* XRD and *in-situ* luminescence measurements should be performed, to obtain information about the mechanism and kinetics of this reaction and the non-incorporated  $\text{Eu}^{3+}$  ions.

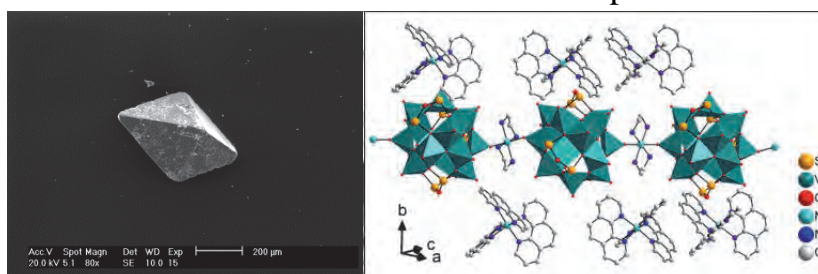


Fig. 1: SEM image (left) and structure of  $[\text{Ni}(\text{phen})_3]_2\{[\text{Ni}(\text{en})_2]\text{V}_{15}\text{Sb}_6\text{O}_{42}\} \cdot 20 \text{H}_2\text{O}$  (right).

[1] K. Y. Monakhov, W. Bensch, P. Kögerler, *Chem. Soc. Rev.*, **2015**, 44, 8443.

[2] M. Wendt, U. Warzok, C. Näther, J. van Leusen, P. Kögerler, C. A. Schalley, W. Bensch, *Chem. Sci.*, **2016**, 7, 2684.

## **Yuriy Potrakhov**

[YN@eltech-med.com](mailto:YN@eltech-med.com)

JSC ELTECH-Med

Department staff of the department of the Electronic Devices in Saint Petersburg Electrotechnical University "LETI"

**Engineer of X-ray equipment**

SPb Prof. Popova 5 lit A

**Research interests:** X-ray radiography in different areas of human activity: medicine, industry, agriculture, etc.



### **Conducting X-ray researches by portable technical equipment in nonspecialized and nonstationary conditions**

As still not defined regulatory framework for medical X-ray diagnostic in unspecialized conditions, such as "at home", the solution of this problem is becoming more acute.

Reasons for conducting X-ray diagnostic studies at home may be different, including:

- somatic "serious" condition in elderly patients who are unable to get to the health facility for suspected pneumonia, fractured limbs, other trauma, etc .;

- availability of financial well-off citizens who do not want to stand in line at the reception, and is therefore ready to pay for X-ray diagnostic, for example, for the purpose of diagnosis and monitoring of inflammatory control in the lungs or the fracture healing process at home.

However, in many cases, X-ray radiography in unspecialized conditions can not be regarded as a method of definitive diagnosis, since there is a number of specific restrictions in carrying out such researches:

- often medical condition of patient does not allow to perform X-ray examination in the standard (at least 2) projections;

- on the size and weight of the X-ray apparatus, X-ray visualisation system and, most importantly, the tripod device;

- on the value of exposure dose of X-rays;

- on the total electric power consumption.

Obviously, the use of traditional stationary tripod devices providing positioning X-ray apparatus relative to the patient, at home is not possible. Therefore, using portable tripods or takes the picture without using a tripod - "in hand." Therefore, special importance becomes the issue of radiation safety for the staff carrying out the study, and to others who may also be involved in the study, such as the laying of the patient. However, the use of stationary means of protection against the unused X-ray radiation, as well as remove others at a safe distance in the home is almost impossible. Therefore it is necessary to use such a technique of X-ray photography, which can significantly reduce the exposure dose of radiation than when using stationary devices. In this case, is extremely important to increase the image quality of the test organ, the necessary and sufficient for a decision on the presence or absence of pathology.

## Elena Povarova

[eipovarova@mail.ru](mailto:eipovarova@mail.ru)

Peoples' Friendship University of Russia

Engineer

Center for Collective Use "Physico-chemical study of new materials, substances and catalytic systems"

6, Mikluho-Maklaya st., Moscow, Russia, 117198

**Research interests:** Heterogeneous Catalysis, XRD study, Surface Properties.



### Crystal structure investigation of ternary sodium-zirconium phosphate with a NASICON type structure

Complex phosphates are solid electrolytes of the **Na-Super-Ionic CONductor (NASICON)**. The basic phosphate is sodium-zirconium phosphate  $\text{NaZr}_2(\text{PO}_4)_3$  (**NZP**). The composition of NZP can be varied by fully or partially replacing sodium or zirconium ions without substantial changes in the crystal structure. The introduction of various ions into NZP offers promise for use it as active and selective catalysts with a microporous structure formed by ionic conductivity channels.

The crystalline framework structure of NZP has a polyhedral group and channels of ionic conductivity. The structure forming B cation is an ion of zirconium, and the anion forming element is a phosphor. The charge of the anionic framework is compensated for by cations:  $\text{Na}^+$  ions that can occupy two positions, **M1** and **M2**, in a channel. At  $\sim 20^\circ\text{C}$ , M1 is completely populated, and M2 is free. Investigations of the properties of the  $\text{NaZr}_2(\text{PO}_4)_3$  show that the temperature anomalies of electric conductivity observed in the  $250\text{--}300^\circ\text{C}$  range are associated with the transition of sodium ions from M1 into M2, as are the unit cell parameters.

In this work we report the synthesis and the characterization of M-NZP powders obtained through the reaction of chlorides.

All samples M-NZP ( $\text{M}^{2+} = \text{Co}^{2+}, \text{Ni}^{2+}, \text{Cu}^{2+}$ ) were synthesized by the sol-gel method [1]. The X-ray data (DRON 3.0M,  $\text{CuK}\alpha$  radiation, Ni filter, angles  $2\theta$  from  $8$  to  $70^\circ$ ) substantiated the structure of NZP. The surface layer composition of NZP was characterized by X-ray photoelectron spectroscopy (XPS).

Thus, XRD spectra of obtained phosphate indicate the provisions of the proximity and intensity of the diffraction peaks with the literature [2]. With growth of the contents of M the volume of the unit cell increases in case of Cu- and the Co-NZP. The XRD showed in all M-NZP availability of dioxide of zirconium  $\text{ZrO}_2$  and a pyrophosphate of zirconium  $\text{ZrP}_2\text{O}_7$ . XPC spectra shows that the composition of the surface layer differed from the stoichiometric. The ratios of P/Zr and O/Zr for  $\text{Na}_3\text{ZrCo}(\text{PO}_4)_3$  sample are overrated by a factor of  $\sim 2$ , indicating an overbalance of phosphate groups on the surface.

[1] E.I. Povarova, A.I. Pylinina, I.I. Mikhaleiko. Catalytic Dehydrogenation of Propanol-2 on Na-Zr Phosphates Containing Cu, Co, and Ni., J. of Physical Chemistry A, 935–941 (2012) 89 (6).

[2] H.Y.-P. Hong Crystal structure and crystal chemistry in the system  $\text{Na}_{1+x}\text{Zr}_2\text{Si}_x\text{P}_{3-x}\text{O}_{12}$ , Mater. Res. Bull., 173- 182 (1976) 11 (2).

## **Alla Pustovalova**

[a.a.pustovalova@yandex.ru](mailto:a.a.pustovalova@yandex.ru)

National Research Tomsk Polytechnic University

**PhD student**

634050 Tomsk, Lenin Avenue, 30, Russia

**Research interests:** X-ray diffraction, X-ray photoelectron spectroscopy, Materials properties



### **Structure and physicochemical properties of N-doped titanium dioxide films**

Physical and chemical properties of materials are investigated generally for understanding of application features in surface modification and structural design. In recent years, titanium dioxide ( $\text{TiO}_2$ ) has attracted lots of interest as an important material for different applications such as solar cells, photocatalysts, self-cleaning and antimicrobial coatings, cosmetics, and biomaterials due to its strong optical absorption, non-toxicity, high chemical stability, biocompatibility, and low cost [1]. It is known that  $\text{TiO}_2$  has three main crystalline phases: brookite with orthorhombic structure and two tetragonal crystal lattices, anatase and rutile. The anatase is known as an effective material for photocatalysis as well as the anatase-rutile mixed structure, while the rutile is more chemically stable in biological liquids and can improve the biocompatibility [1,2]. The anatase or rutile phase formation depends on the method and conditions of deposition.

Reactive magnetron sputtering is one of the most attractive techniques providing more benefit in controlling the properties, structure and composition of  $\text{TiO}_2$  films [3]. The phase transition can be attained by using the nitrogen addition during deposition process. A number of studies are focused on nitrogen incorporation and determination of its state in the film structure [1,2,4].

This work presents the study results of nitrogen doping effect on  $\text{TiO}_2$  films structure prepared by the reactive magnetron sputtering deposition. Phase structures of the films were examined by X-ray diffraction and Raman scattering. The surface morphology was observed with atomic force microscopy. Chemical bonds and composition of N- $\text{TiO}_2$  films were determined using X-ray photoelectron spectroscopy with monochromatic Al-K X-ray source.

- [1] A. Pustovalova, et al., Key Eng. Mater. 383–388 (2016) 683.
- [2] R. Gago, et al., Mater. Chem. Phys. 729–736 (2012) 136.
- [3] J. Zheng, et al., Surf. Coatings Technol. 293–300 (2014) 240.
- [4] J. Ananpattarachai, et al., J. Hazard. Mater. 253–261 (2009) 168.

## **Salim Reza**

[salim.reza@miun.se](mailto:salim.reza@miun.se), [salim.reza@desy.de](mailto:salim.reza@desy.de)

Mid Sweden University and Deutsches Elektronen-Synchrotron (DESY)

**PhD researcher**

Holmgatan 10, 851 70, Sundsvall, Sweden

**Research interests:** Radiation Detectors, Phase-contrast Imaging,  
Detector Simulations



### **Monte Carlo and FEM Simulation of a Monolithic Active Pixel Sensor**

The new generation of X-ray Free Electron Laser (XFEL) sources are capable of producing light beams with billion times higher peak brilliance than that of the best conventional X-ray sources available today. This advancement motivates the scientific community to push forward the existing technology to its limit, in order to design photon detectors which can cope with the extreme flux generated by the XFELs. Sophisticated experiments like deciphering the atomic details of viruses, filming chemical reactions or investigating the extreme states of matter require detectors with high frame rate, good spatial resolution, high dynamic range and large active sensor area.

In this work, Monte Carlo algorithm based Geant4 and Finite Element Method (FEM) based Synopsys Sentaurus TCAD toolkits have been used to simulate, respectively, the X-ray energy deposition and the charge sharing in such a detector. The detector is based on Monolithic Active Pixel Sensor (MAPS) technology. Energy deposition per pixel and charge sharing between adjacent pixels at different energies have been investigated.

## **Janina Roemer**

[Janina.Roemer@physik.lmu.de](mailto:Janina.Roemer@physik.lmu.de)

Faculty of Physics & CeNS, Ludwig-Maximilians-Universität München

**PhD student**

Geschwister-Scholl-Platz 1, 80539 Munich, Germany

**Research interests:** Organic and perovskite photovoltaics, investigation of crystallite size and disorder and their relation to optical and electronic properties



### **Tuning and characterizing structural properties of organic semiconductors and organometal halide perovskites**

Organic and perovskite solar cells are promising candidates for low-cost photovoltaic devices. In both classes of materials optical and electronic properties are closely related to structure at the nanoscale. An experimental investigation of this relation requires sample preparation methods which allow for tuning crystallinity and crystallite sizes, as well as appropriate techniques to characterize these properties.

Using molecular beam deposition, we are able to control crystallinity and size of C<sub>70</sub>-aggregates grown on pentacene thin films by the choice of evaporation rate and sample temperature. This provides us with an adjustable model system with well defined interfaces between the two semiconductors, which is required for investigation of charge carrier separation in organic solar cells. Crystal structure and degree of order of the fullerene have been investigated by X-ray Bragg scattering in reflection and grazing incidence geometry at beamline P08 at PETRA III (DESY).

Quantum size effects in organometal halide perovskites are currently subject of intense research, as they can be used to tailor the optical properties of the material. The Linz Institute for Organic Solar Cells together with the Department of Soft Matter Physics of the Johannes Kepler University Linz developed a method to infiltrate nanoporous silicon with perovskite, achieving blue-shifted photoluminescence. We investigated the distribution of crystallite sizes over the thickness of the porous layer by micro-focus high energy X-ray depth profiling at beamline P07 at PETRA III (DESY).

**Irina Safiulina**

[irina.safiulina@gmail.com](mailto:irina.safiulina@gmail.com)

PNPI

**Laboratory assistant**

Orlova Roscha, Gatchina, Leningrad district, 188300, Russia

**Research interests:** small-angle neutron and x-ray scattering, fractal structures, helical magnetic structures



## Investigation of the mesostructure of $Mn_{1-x}Co_xGe$ compounds synthesized under high pressure

Samples of  $Mn_{1-x}Co_xGe$  solid solutions have been synthesized by the high pressure method at the Institute for High Pressure Physics, Troitsk, Moscow Region, Russia. As they can be only synthesized under high pressure, the samples are in a polycrystalline powder form with crystallite size not less than 10 micron (see [1] for details). The X-ray powder diffraction confirmed the B20 structure of these samples. The measurements of the mesostructure of MnGe compound by means of the small-angle neutron scattering method have shown presence of the strong nuclear scattering in the  $Q$ -range  $[0.007 - 0.2] \text{ \AA}^{-1}$ . This scattering is described by the law  $Q^{-n}$  with  $n$  equal to 3. The SANS measurements performed in the  $Mn_{1-x}Co_xGe$  solid solutions (SANS-1, MLZ, Munchen) showed that the nuclear mesostructure does not change with the Co-doping.

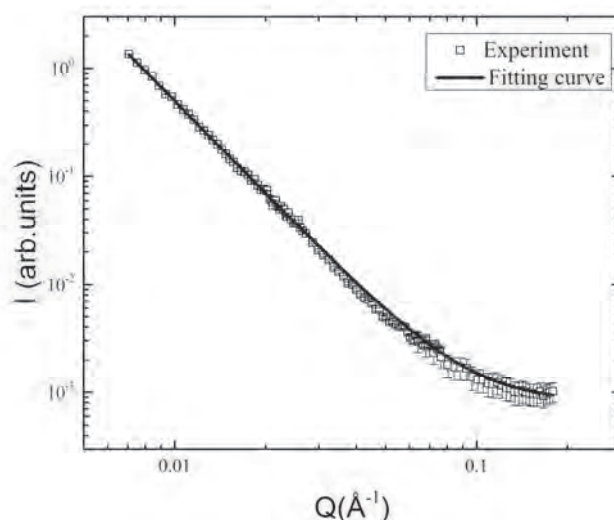


Fig.1 Small-angle neutron scattering intensity versus momentum transfer for MnGe. The data are well fitted with the power law  $Q^{-n}$ , with exponent value  $n = 3$ .

The scattering law  $Q^{-3}$  can be explained as a result of the complex synthesis process that provides a logarithmical dependence of density of defects in mesostructure of samples. This exponent  $n=3$  corresponds to the logarithmic spatial pair correlation function  $\gamma(r) \sim \ln(\xi/r)$ . The correlation function increases with an additive rather than multiplicative constant upon reducing the scale length by a fixed rescaling factor. This leads to a logarithmic law instead of the usual power law for fractals. The nature of this scattering remains unknown, while the knowledge on the mesostructure can be crucial in understanding and controlling of the magnetic properties of B20 solid solutions grown under high pressure.

[1] A. V. Tsvyashchenko, J. Less-Common Met. 99, L9 (1984)

**Martin Seyrich**

[martin.seyrich@desy.de](mailto:martin.seyrich@desy.de)

**PhD Student**

DESY, Hamburg, Germany

**Research interests:** Ptychography, Nano Probe Applications,  
Interferometric Distance Measurement



## **Laser-Interferometric Position Measurement for High-Resolution 3D Ptychography**

Ptychography is a coherent scanning microscopy technique which enables spatial resolutions beyond the focus size of the probe beam. In this case, the resolution may only be limited by the accuracy of the scan positions themselves [1]. Laser Interferometry offers contact-free distance sensing with sub-nanometer resolution. In the ptychographic algorithm, this position information can be used to correct artifacts caused by vibrations, motor inaccuracies or thermal drifts.

The necessary rotational degree of freedom for 3D ptychography poses a challenge to the design of the reflector optics, which is solved by using partially-coated high-index ball lenses [2]. With this approach, we hope to achieve 10nm spatial resolution in 3D on a regular basis in the future.

[1] Faulkner, H. M. L., & Rodenburg, J. M. (2005). Error tolerance of an iterative phase retrieval algorithm for moveable illumination microscopy. *Ultramicroscopy*, 103(2), 153-164.

[2] Seyrich, K. M. (2015). An Interferometric Positioning System for High-Resolution 3D Ptychography. Master's Thesis, TU Dresden.

## Ivan Shishkin

[shishkin@lns.pnpi.spb.ru](mailto:shishkin@lns.pnpi.spb.ru)

Petersburg Nuclear Physics Institute

Junior researcher

[dir@pnpi.spb.ru](mailto:dir@pnpi.spb.ru)

**Research interests:** Small-angle neutron and X-ray scattering, SQUID-magnetometry, Ferromagnetic resonance



### Defects of the crystalline structure of inverse opals

Inverse opal-like structure (IOLS) were obtained by filling the voids of opal synthesized from polystyrene microspheres with a diameter of  $540 \pm 10$  nm, are stacked in a close packing with a face-centered cubic (FCC) structure. After dissolution of the microspheres in the toluene formed an ordered porous materials. Master and PhD students of the faculty of Material Sciences of Moscow State University carried out synthesis of samples.

By method of ultra small-angle X-rays diffraction (USAXS) was shown that impossible to grow an IOLS films with perfect FCC structure [1-3]. The imperfection of the crystalline structure of IOLS based on Co was studied by USAXS, using a films with a thickness of  $n = 0.5, 2, 7, 17, 20$  and  $26$  layers, where one layer corresponds to close-packed polystyrene microspheres in a hexagonal order.

The experiments were performed at BM-26@ESRF (DUBBLE) with the photon energy  $13$  keV ( $\lambda = 1.033$  Å) and a compound of 7 refractive beryllium focusing lenses, in order to have high resolution. Sample to detector distance was about 7 meters. Photonic Science Detector with pixel size of  $22.7 \times 22.7 \mu\text{m}^2$  was used for diffraction maps capturing. Initially the samples were mounted so that the substrate was perpendicular to the beam. Vertical axis corresponded to the direction of meniscus moving at the stage of OLS synthesis. In order to determine a type of packing we have performed angle scans around vertical axis in range  $[-65^\circ \div +65^\circ]$  ( $\omega$ -scans, where  $\omega = 0^\circ$  is initial position) with step of  $1^\circ$ . In reciprocal space except for the diffraction peaks corresponding to FCC structure was observed in the diffraction rods, corresponding to the contravention in alternating layers along the crystallographic axis [111].

The dependence of the integral intensity distribution along the rods for different thicknesses of the samples showed that with increasing number of layers the number of rods is not reduced, which indicates the imminent appearance of structural defects in the growth process. It is experimentally shown that the FCC structure can not be displayed in the samples with a small number of layers ( $n < 7$ ). Found that most opal-like crystals and derived from it inverse opals with  $n \geq 7$  only of 66% are composed of FCC crystallites.

This work was supported by Russian Foundation for Basic Research. № 14-22-01113.

[1] N.A. Grigoryeva, et. al., Phys. Rev. B. 064405 (2011) 84

[2] A.K. Samusev, et. al., Physics of the Solid State. 1946-1955. (2012) 10

[3] A.V. Chumakova, et. al., Phys. Rev. B. 114103 (2014) 90

## Dmitrii Shuleiko

[shuleyko.dmitriy@physics.msu.ru](mailto:shuleyko.dmitriy@physics.msu.ru)

Lomonosov Moscow State University

PhD student

1/2 Leninskie Gory, Moscow, 119991, Russia

**Research interests:** femtosecond laser radiation, amorphous silicon, photoluminescence, surface periodic structures, silicon nanocrystals



### **Anisotropy of structural and electrical properties of amorphous silicon films processed by femtosecond laser radiation**

Femtosecond laser pulses with high emission intensity and low photon energy can help to achieve uniform nanostructuring and modification over the entire volume of siliceous films [1], as well as anisotropy of their structural, electrical and optical properties. For example, surface periodic structures can be formed [2]. Femtosecond laser radiation also can be used to improve the properties of amorphous hydrogenated silicon films (a-Si:H) for potential applications in photovoltaics.

In this paper, a-Si:H films were processed by femtosecond laser pulses (1250 nm, 100 fs, spot diameter 150  $\mu\text{m}$ ) in raster mode. Scanning electron microscopy revealed the presence of the one-dimensional grating-like structure with a period of about  $0.36 \pm 0.03$  or  $1.11 \pm 0.05$   $\mu\text{m}$  on the treated surface, perpendicular to polarization of the incident beam. This result is in agreement with the data of [3].

Electrical measurements have shown that the conductivity of a-Si:H film after irradiation with femtosecond laser pulses increased up to 3 orders of magnitude (Table 1) due to dehydrogenation and nanocrystallization of the film [4].

Sample	Specific conductivity $\sigma$ ( $\Omega \cdot \text{cm}$ ) <sup>-1</sup>
Processed area, the contacts are parallel to scan lines and surface periodic structures	$1.58 \cdot 10^{-6}$
Processed area, the contacts are perpendicular to scan lines and surface periodic structures	$4.48 \cdot 10^{-6}$
Amorphous silicon	$6.73 \cdot 10^{-9}$

Table 1. Conductivity of a-Si:H film before and after femtosecond laser irradiation.

The conductivity along the scan lines and periodic structures is almost threefold greater than in the perpendicular direction. This effect can be explained by non-uniform crystallization of amorphous silicon, and the electric field anisotropic depolarization inside the surface periodic structure.

[1] A. V. Emelyanov, M. V. Khenkin, A. G. Kazanskii, et al. *Thin Solid Films* 410–413 (2014) 556

[2] G.A. Martynovskiy, G.D. Shandybina, Yu.S. Dementeva et al. *Semiconductors* 1339–1345 (2009) 43

[3] R. Drevinskas, M. Beresna, M. Gecevičius et al. *Appl. Phys. Letters* 171106 (2015) 106

[4] A.V. Emelyanov, A.G. Kazanskii, P.K. Kashkarov et al. *Semiconductors* 769–774 (2012) 46

**Dmitri Smirnov**

smirnovdim@gmail.com

<sup>1)</sup>LPI RAS, <sup>2)</sup>MIET

**Researcher**

<sup>1)</sup> 53 Leninskiy Prospekt, Moscow, Russia, 119991

<sup>2)</sup> 1 Shokin Sq., Zelenograd, Moscow, Russia, 124498

**Research interests:** x-ray analytical methods, thin-film nanostructures,  
micro- and nanoelectronics



## **Combined X-ray Measurements for Micro- and Nanoelectronic Technologies**

The set of the combined X-ray methods for the multipurpose two-wavelength reflectometer is discussed. It was first implemented a relative measurement mode by determining a ratio of signals on two or more selected spectral lines [1]. This approach eliminates the instrument error and enables correct measurements at grazing-incidence angles.

The developed comprehensive approach for the measurement of multilayer thin-film nanostructures provides the use of complementary research methods which are based on different physical principles and allow to resolve ambiguities in the solution of inverse problems [2]. X-ray reflectometry is a standard for the study of multilayer thin-film structures; however, the analysis only of the specular reflection does not allow to separate the contributions from the density gradient of layer materials and from the interface roughness. In this regard, refractometry and diffuse X-ray scattering are combined along with relative reflectometry.

The most important source parameter for X-ray measurements is a focus size. The system is equipped with a fine-focusing X-ray source with a focus projection of  $\sim 10 \mu\text{m}$ . It provides a high angular resolution and allows to use X-ray refractometry for the study of multilayer nanostructures in practice.

The specified X-ray optical scheme also provides a study of two different areas of diffuse X-ray scattering during one measurement which increases the accuracy and uniqueness of the analysis. The presented complex of methods permits to resolve the ambiguities such as the “density – roughness” of the reflectometry inverse problem and to calculate parameters of buried layers in investigated structures.

A special attention is also paid to the correctness of the solution of inverse problems [3]. The regularization of experimental data in order to reduce an error when working with a ratio of the signals and the stochastic algorithms for the fitting of the theoretical and experimental curves is used.

Combined X-ray measurements have been tested on the nanoelectronic solid-state structures such as diffusion-barrier TiN/Ti layers and low-k dielectrics. The possibility of the accurate determination of the physical parameters of hidden and buried layers formed in the investigated structures during multistage manufacturing processes is studied.

[1] A.G. Touryanski, et al. X-ray reflectometer. USA Patent No. 6041098, US Cl. 378–70 (2000).

[2] D.I. Smirnov, et al. Technical Physics Letters. 39(7), 640–643 (2013).

[3] A. Benediktovitch, et al. *Theoretical Concepts of X-Ray Nanoscale Analysis*. (Springer, 2014).

## **Roman Sundeev**

[apricisvir@gmail.com](mailto:apricisvir@gmail.com)

FSUE "Central Research Institute of Ferrous Metallurgy  
named after I.P. Bardin"

**Senior Researcher**

105005, Moscow, st. Radio 23/9

**Research interests:** severe plastic deformation; synchrotron X-ray diffraction; amorphous state



### **Synchrotron X-ray diffraction study of the local structure amorphous phases obtained in Ti-Ni-Cu alloy using different approaches**

The method of melt quenching is most effective for the realization of an amorphous state in metal alloys [1]. However in recent years the severe plastic deformation (SPD) of crystalline metallic materials has been used for production of amorphous state [2,3].

The structure of amorphous  $\text{Ti}_{50}\text{Ni}_{25}\text{Cu}_{25}$  alloy was investigated upon high-pressure torsion (HPT). Amorphous  $\text{Ti}_{50}\text{Ni}_{25}\text{Cu}_{25}$  alloy fabricated by melt quenching in an argon atmosphere was chosen for this study. Several cyclic amorphous state–crystal phase transitions were found earlier in this alloy upon HPT [4]. The samples were deformed by high-pressure torsion under the same conditions at a hydrostatic pressure of 4 GPa and at room temperature. The rotation velocity of the movable anvil was about 0.67 rpm. The total number of movable anvil rotations  $n$  was changed from 1/4 to 9. The initial thickness of samples was 50  $\mu\text{m}$ . Various diffraction methods (spatially resolved synchrotron X-ray diffraction, transmission electron microscopy and classic X-ray analysis) were applied for investigating the evolution of structural parameters of alloy. This enabled us to obtain the dependences of average and local fractions of crystalline phase along the sample radius with a step of 500  $\mu\text{m}$  on the deformation. The radial distribution functions allowing calculations of the interatomic distance and coordinate number in several coordinate shells of an investigated sample were obtained from the local X-ray patterns recorded at each point along the sample's radius. Based on our results, we conclude that the amorphous state in the  $\text{Ti}_{50}\text{Ni}_{25}\text{Cu}_{25}$  system obtained by deformation-induced amorphization at room temperature upon HPT was identical to the one that emerges upon melt quenching.

[1] F.E. Luborsky (Ed.), *Amorphous Metallic Alloys*, Butterworths, London, 1983

[2] A.P. Zhilyaev, T.G. Langdon, *Prog. Mater. Sci.* 893-979 (2008) 53

[3] R.V. Sundeev, A.M. Glezer, A.V. Shalimova, *J. Alloys Comp.* 292-296 (2014) 611

[4] R.V. Sundeev, A.M. Glezer, A.V. Shalimova, *Mat. Lett.* 32-34 (2014) 133

**Olesya Timaeva**

[gertrudejames@mail.ru](mailto:gertrudejames@mail.ru)

Moscow Technological University

**PhD student**

86 Vernadsky prosp., Moscow, 119571, Russia

**Research interests:** solid state chemistry, synthesis of nanoparticles, titanium dioxide, X-ray powder diffraction



### **Interdisciplinary approach in studying of composites based on "smart" polymers with functional inorganic particles**

Now the most perspective way of the scientific direction is the interdisciplinarity as in the choice of objects to study combining amorphous substances with inorganic nanocrystals and crystals, and in the appeal to different areas of knowledge (chemistry, biology, crystallography, physics, mathematics) and different investigation methods (physical, chemical, physico-chemical). In this regard, it seems promising from scientific and practical view points to synthesize by several methods (mechanical trituration - *method 1*, physical precipitation – *method 2*, mechanical activation by ball milling – *method 3*, the synthesis of particles in the presence of poly-N-vinylamides' aqueous solutions - *method 4*) and characterize by complex methods nanocomposites based on poly-N-vinylamides (poly-N-vinylcaprolactam - PVCL, poly-N-vinylpyrrolidone) with functional particles (lanthanum nitrate hexahydrate) and nanoparticles (oxides of titanium (IV) - anatase,  $\eta$ -modification) and study their bactericidal and photocatalytic properties. This was the aim of this study.

According to wide-angle X-ray scattering the preparation of nanocomposites by *methods 1* and *3* leads to changes in NT/PVCL system: mechanical cracking, hydration and dehydration of the polymer; phase and polymorphic transitions, changes of crystallinity degree of NT particles. The results of small-angle X-ray scattering indicate that the mechanical activation of PVCL and NT powders by ball milling increases the size of the nanoparticles upon transition from mechanically ground to mechanoactivated, while decreasing of duration and speed of a mechanical ball-milling (*method 3*) reduces the size of the nanoparticles in NT/PVCL nanocomposites. It was found that composites  $\text{La}(\text{NO}_3)_3 \cdot 6\text{H}_2\text{O}/\text{PVCL}$  (*method 1*) and nanocomposites NT/PVCL (*methods 1* and *3*) have bacteriostatic properties against microorganisms *Staphylococcus aureus*, *Escherichia coli*, *Candida albicans*.

The preparation of nanocomposites by physical precipitation (*method 2*) allows to stabilize the NT particles in the solution. The particles show higher catalytic activity under UV irradiation in the photodestruction reaction of methyl orange compared with the samples obtained by other methods. Based on the results of scanning electron microscopy, NT nanoparticles in nanocomposites NT/PVCL are located inside the polymer globule, so these nanocomposites do not exhibit any bactericidal properties.

It was established by wide-angle X-ray scattering that the titanium dioxide particles synthesized in the presence of poly-N-vinylamides (*method 4*) are a mixture of two nanosized phases (anatase and  $\eta$ -modification) and the X-ray amorphous polymer. IR spectroscopy and element analysis showed that the polymer content in nanocomposites is about 11-20%. These samples have high antibacterial activity against the microorganisms *Staphylococcus aureus*, *Escherichia coli*, *Candida albicans*.

The original programs for treatment and calculation of diffraction patterns with amorphous and nanosized objects and for correlation of absorption bands of IR spectra of the studied samples with standards have been created.

## **Gennadiy Timofeev**

[gennady92@gmail.com](mailto:gennady92@gmail.com)

Saint-Petersburg Electrotechnical University

**PhD student**

Professora Popova 5, 197376 St. Petersburg, Russian Federation

**Research interests:** Medicine, Photo X-ray Tube appliances, electrical circuit engineering.



### **X-ray Tube with photocathode. Advantages and applying**

Radiographing a moving object requires a source of pulsed X-ray radiation. The most common types of impulse X-ray tube are X-tube with cold cathode and an X-tube with thermo cathode, which has third electrode, called “the greed”. But there are other types of pulse X-ray tubes. For example, Photo X-Tube which is the combination of photomultiplier tube and an ordinary X-ray tube.

Comparing the photo x-tube with other pulse tubes in high frequency range, the choice is depend on such requirements as the x-ray intensity (tube current) in conjunction with its stability. The photo X-tube provides excellent repeatability of the output intensity of the X-ray radiation, but has a medium pulse current (up to several mA). Whereas the tube with field emission has extremely high peak currents (up to  $10^3$  A), but the radiation stability varies greatly from pulse to pulse. In addition, it is worth noting that the term of cathode lifetime limited by several thousands of pulses. Whereas the photocathode lifetime is approx. several thousands of hours. The output x-ray intensity of the photo and carbon-based cathodes are approximately equals, but the photocathode has a quite better frequency characteristic.

Thus, there are several major application areas for the photocathode X-ray tube. The first one is the scintillator relax time examination as it is highly important to have stability of x-ray repetitive pulses as well as the ability of high frequency x-ray modulation. The second one is radiographing of the fast processes, such as: explosions, collisions. However, in this field it is possible to process obtained pictures on the computer instead of using stable X-ray source.

Another promising field is the usage of the photo X-tube in tomography. Nowadays, exiting devices have come to its limit characteristics on several fronts: firstly, the inability to further reduces the tube pulse time and second one is the inability to further increase the speed of rotation of the X-tubes due to high centripetal acceleration. In these conditions a person needs to lie still. But pictures of moving organs, such as a heart, can be obtained of unacceptable quality. In such circumstances the usage of photo X-tube could give impetus to further development of CT scanners. However, for usage in this field the X-ray tube with a photocathode needs to be improved in the power characteristics, such as tube current is.

**Elena Ushakova**  
[ushelen1171@gmail.com](mailto:ushelen1171@gmail.com)  
“Dubna” University

**Student**

Dubna, Universitetskaja st.,18

**Research interests:** Neutron Reflectometry , Electrochemistry, Nuclear Research



### **Operando Neutron Reflectometry study of lithium deposition in lithium metal batteries**

Elena Ushakova<sup>1</sup>, Alexey Rulev<sup>2</sup>, Elmar Kataev<sup>2</sup>, Igor Gapon<sup>3</sup>, Viktor Pterneko<sup>3</sup>, Daniil Itkis<sup>1,2</sup>, Mihail Avdeev<sup>3</sup>

Dubna University, Dubna, Russia Lomonosov Moscow State University, Moscow, Russia Joint Institute for Nuclear Research, Dubna, Russia

At present rapidly evolving technologies require continuous enhancement of energy storage performance and creation of next-generation high-energy and high-power batteries. Lithium metal is considered to be the most perspective anode material for the rechargeable lithium battery systems including highly promising Li–sulfur, Li–air, and others [1-3]. Main reason preventing successful deployment of rechargeable lithium metal batteries is connected with non-uniform lithium plating during charge. Li is deposited in the form of filaments often called “dendrites” at negative electrode that leads to internal short-circuiting, low Coulombic efficiency, and short cycle life. Although there is still no widely acknowledged mechanism of dendrite initiation and propagation established.

Dendrite formation during electrodeposition is rather complicated process and can't be studied with only electrochemical techniques. *Hence*, in order to monitor solid electrolyte interphase (SEI) formation, dendrite nucleation and growth in polymer electrolyte we suggest using neutron reflectometry (NR) *in situ* as transient processes taking place in the working electrochemical cell can hardly be quenched for *ex situ* analysis. In contrast to *other techniques*, NR provides an averaged information of surface layers evolution thus allowing to avoid locality of information obtained, which can be distorted by many factors.

NR measurements of operating electrochemical cells have been performed in originally designed three electrode electrochemical cell at GRAINS reflectometer with horizontal sample plane (IBR-2 reactor, Dubna). Copper coated on single-crystal Si substrate (with Ti adhesion sublayer) served as a working electrode, Li-foil fixed to Ni mesh current collector – as a counter electrode. Ag+/Ag reference electrode in Vycor-frit isolated tube was inserted into the cell for providing accurate potential measurement. For contrast optimization the electrolyte with deuterated propylene carbonate solvent (1M LiClO<sub>4</sub> in PC-d<sup>6</sup> (C<sub>4</sub>D<sub>6</sub>O<sub>3</sub>)) was used in the experiments. Reflectivity data were collected under open circuit potential (OCV to -0.5V vs. Li<sup>+</sup>/Li) after lithium was deposited on the working electrode upon various amount of charge passed through the cell at the rate of the deposited layer thickness up to 200 nm. Fit analysis of the obtained dataset shows the technique of neutron reflectometry allows to detect surface layers covering the electrode of about few nanometers thick, further provides with an estimate averaged roughness of the deposited layers.

[1]. Zhong Ma, Xianxia Yuan. A Review of Cathode Materials and Structures for Rechargeable Lithium-Air Batteries. *Energy Environ. Sci.*,140, (2015) 15.

[2]. G. Bieker, M. Winter. Electrochemical in situ investigations of SEI and dendrite formation on the lithium metal anode. *Phys.Chem.Chem.Phys.*, 8670 (2015) 17.

[3]. Wu Xu, Jiulin Wang. Lithium metal anodes for rechargeable batteries. *Energy Environ. Sci.*, 515 (2014) 7.

**Gleb Valkovskiy**  
Valkovsky\_Gleb@mail.ru  
Saint Petersburg State University

**Research assistant**

7/9 Universitetskaya nab., St. Petersburg, 199034 Russia.

**Research interests:** Synchrotron techniques, X-ray diffraction,  
Relation between crystal structure and magnetism



## **Variation of interatomic distances in MnGe under temperature and pressure**

The silicides and germanides of Mn, Fe, Co with a B20 crystal structure have surprisingly various magnetic and electronic properties [1]. Besides, their properties are remarkably temperature- and pressure- dependent.

The B20 phase has space group  $P2_13$ , which is cubic but of rather low symmetry. In the so-called ideal B20 structure the nearest neighbor coordination of each atom is seven equidistant atoms of the opposite kind [2]. These seven atomic sites lie on seven of the twenty vertices of a pentagonal dodecahedron centered on the atom. Interestingly, none of the abovementioned silicides and germanides has the ideal B20 structure, the atoms are slightly shifted from their ideal positions. This results in splitting of the 7 bonds into 3 the longest, 3 medium and 1 the shortest. Though the difference in the bond length is small, the distortion of the structure from its ideal form is supposed to have an essential effect on physical properties.

In this series, MnGe has exceptionally broad transition from helix to paramagnetic state in the range of  $\sim 150 - 300$  K [3, 4]. In addition, spin transition from high spin to low spin state is reported to occur under pressure [5]. Yet, the peculiar correlation between magnetic and structural properties of MnGe remains poorly understood.

Here single crystal synchrotron diffraction studies of atomic coordinates and interatomic distances as a function of temperature and pressure were carried out. It was revealed that the longest Mn-Ge distances have peculiar behavior. They extend faster with temperature than the others within the transition from helix to paramagnet. Though, under pressure they started to reduce more rapidly after the pressure of  $\sim 10$  GPa is released, i.e. in the low spin state.

[1] J.F. DiTusa, et al., Phys. Rev. B. 144404 (2014) 90

[2] L.F. Mattheiss, et al., Phys. Rev. B. 20 (1993) 47

[3] E. Altyntsev, et al., Phys. Rev. B. 174420 (2014) 90

[4] M. Deutsch, et al., Phys. Rev. B. 144401 (2014) 90

[5] M. Deutsch, et. al., Phys. Rev. B. 180407(R) (2014) 89

## Polina Vanina

[p.yu.vanina@gmail.com](mailto:p.yu.vanina@gmail.com)

Peter the Great Saint-Petersburg Polytechnic University

PhD student

Russia, 195251, St.Petersburg, Polytechnicheskaya, 29

**Research interests:** Physics of solid state, physics of functional dielectric materials, including ferroelectrics, antiferroelectrics, relaxor materials



## Dielectric and magnetic properties of $\text{La}_{0.875}\text{Sr}_{0.125}\text{MnO}_3$ and $\text{La}_{0.93}\text{Sr}_{0.07}\text{MnO}_3$ in high magnetic fields

P.Yu. Vanina<sup>1</sup>, A.A. Naberezhnov<sup>1,2</sup>, V.I. Nizhankovskii<sup>3</sup>, R.F. Mamin<sup>4</sup>

<sup>1</sup>Peter the Great Saint-Petersburg Polytechnic University, Saint-Petersburg

<sup>2</sup>Ioffe institute, Saint-Petersburg

<sup>3</sup>International laboratory of high magnetic fields and low temperatures, Wroclaw

<sup>4</sup>Kazan E. K. Zavoisky Physical-Technical Institute, Kazan

The aim of this study was to obtain information about the values of the magnetic moments, types phase transitions and temperatures for compositions  $\text{La}_{0.93}\text{Sr}_{0.07}\text{MnO}_3$  (LSMO-0.07) and  $\text{La}_{0.875}\text{Sr}_{0.125}\text{MnO}_3$  (LSMO-0.125). The experiment was performed on a vibration magnetometer at the International Laboratory of High Magnetic Fields and Low Temperatures (Wroclaw, Poland).

In order to accurately determine the temperature of the phase transition temperature dependence of magnetization of the samples was approximated by various functions in a low-temperature and high-temperature areas. The low-temperature phase was approximated by function  $(T_C - T)^\beta$ , from which we obtained the values of the critical exponents  $\beta = 0,280 \pm 0,0084$  for the composition LSMO-0.07 and  $\beta = 0.440 \pm 0.0132$  for LSMO-0.125, as well as the phase transition temperatures  $T = 125.8 (1.5) \text{ K}$  (LSMO-0.07) and  $T_1 = 181.2 (1.5) \text{ K}$  and  $T_2 = 157.6 (1.5) \text{ K}$  (LSMO-0.125).

Paramagnetic phase was approximated in accordance with the function:  $1/M = (k_B T)/(N\mu^2 B)$ , where  $\mu$  - magnetic moment,  $M$  - magnetization,  $B$  - applied magnetic field in oersteds,  $k_B$  - Boltzmann constant,  $N$  - the number of magnetic atoms in unit volume. Thus, the estimated values of the magnetic moments for two compounds:  $\mu_1 = 2,47 (1) \mu\text{B} / \text{Mn}$  and  $\mu_2 = 2,82 (1) \mu\text{B} / \text{Mn}$ , for LSMO-0.125 and LSMO-0.07 respectively.

The obtained information will help clarify the microscopic mechanisms of the processes occurring at approaching the phase transitions, as well as the processes that determine the very high values of the dielectric constant, colossal magnetoresistance and magnetocapacitance effect.

## **Torsten Veltum**

[torsten.veltum@hhu.de](mailto:torsten.veltum@hhu.de)

Institute of Applied Physics

**PhD student**

Heinrich-Heine-University, Universitätsstr. 1, 40225 Düsseldorf,  
Germany

**Research interests:** thin films of Fe, Ni, and Co, magnetic linear dichroism, scanning tunneling microscopy, nanoparticles on thin films and single crystals as well as nanopatterned surfaces



## **Magnetic linear dichroism of 3d metal thin films**

Magnetic linear dichroism in the angular distribution of photoelectrons (MLDAD) is a technique that allow the study of both the electronic band structure and magnetic properties of thin films and single crystals. We are interested in the magnetic properties of the magnetic linear dichroism of 3d metals.

The studied system is epitaxially grown Co(0001) and Fe(110) thin films on a W(110) surface. In this study we use linearly polarized synchrotron radiation in the VUV regime. All measurements are performed at beamline 5, DELTA Dortmund, Germany. The experimental setup includes low-energy electron diffraction (LEED) and angle-resolved photoemission spectroscopy (ARPES). We prepare Co and Fe thin films with a thickness of 20 ML on top of a W(110) single crystal using physical vapor deposition at a pressure better than  $3 \times 10^{-10}$  mbar. The tungsten single crystal is cleaned using the usual cycle of annealing in oxygen atmosphere at 1200 K and subsequent flashes to up to 2300 K [1].

The is a crucial geometry to observe a MLD signal. The sample is magnetized along the y-axis. For Fe thin films the easy magnetization axis lies in-plane along the [1-10] direction. For a thin Co film the easy magnetization axis in-plane is the [1-100] direction. For thicker films the easy magnetization rotates out of plane for Co, and in-plane to the [001] direction for Fe. Light impinges on the surface in the xz-plane and is linearly polarized in it. The detector is positioned at normal emission in z-direction.

Theoretical calculations for these systems make use of dynamical mean-field theory (DMFT) and 3BS many-body calculations, including a complete calculation within the one-step model (1SM) of photoemission, using the local spin-density approximation (LSDA) [2,3].

Our results are compared to previous results of J. Bansmann et al. [4].

[1] M.Bode et al., *Surf. Sci.* **601**, 3308 (2007).

[2] J. Sánchez-Barriga et al., *Phys. Rev. B* **85**, 205109 (2012).

[3] J. Sánchez-Barriga et al., *Phys. Rev. B* **82**, 104414 (2010).

[4] J. Bansmann et al., *Surf. Sci.* **352**, 898 (1996).

## **Egor Vezhlev**

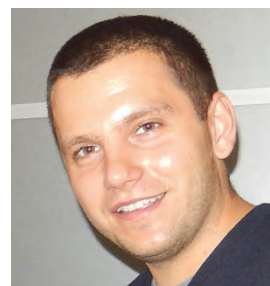
[e.vezhlev@fz-juelich.de](mailto:e.vezhlev@fz-juelich.de)

Jülich Centre for Neutron Science at Heinz Maier-Leibnitz Zentrum

MLZ Forschungszentrum Jülich GmbH

**Postdoctoral Researcher**

Lichtenbergstr. 1 85748 Garching Germany



**Research interests:** Analytical methods for energy materials research  
Neutron depth profiling

### **Neutron depth profiling at the focused neutron beam of MARIA: towards studies of lithium transport in thin film batteries**

Neutron depth profiling (NDP) allows for the determination of the in depth distribution of an appropriate light elements in a few micrometers of solids. It is based on the energy analysis of charged particles produced upon the capture of thermal (cold) neutrons by some light isotopes with a large neutron cross-section. This technique is the method of choice for studies of Li transport in all-solid-state thin film microbatteries. However, the required high depth resolution and high counting rates can only be achieved at the high flux neutron facilities. We have recently built a new multiple detector NDP setup designed for the focused neutron beam of reflectometer MARIA (MLZ) that will allow us to do fast NDP measurements on less than a minute rate. This paves the way to *in situ/ in operando* studies of Li transport and makes exploring the fast battery dis/charging and the battery degradation in time possible.

## Oksana Yurkevich

[oyurkevich@innopark-kantiana.ru](mailto:oyurkevich@innopark-kantiana.ru)

I. Kant Baltic Federal University

**PhD student**

Nevskogo str. 14, Kaliningrad, Russia

**Research interests:** Protective coatings, oxide thin film formation and characterization, synthesis of 3D conformal films by atomic layer deposition, development of the ALD tools.



### Protective Al<sub>2</sub>O<sub>3</sub> coatings for beryllium optics

Beryllium has large benefits for application in X-Ray optics in comparison to other materials, but there are few concerns due to its toxicity and high cost. Besides, usage of X-Ray optical elements at the synchrotron facilities under the powerful irradiation could cause damage of the elements. In this work, we propose the way to elongate the lifetime of Be optics and buildup an additional protection for users by applying thin (~70 nm) alumina oxide coatings. Atomic Layer Deposition (ALD) method has been chosen as the most promising technique for this task, as it provides conformal coatings even on high aspect ratio objects.

Stability tests of the structures were performed under the extreme conditions of the white beam irradiation at the ID06 of European synchrotron Facility (ESRF). Samples were exposed under the synchrotron irradiation at the different environment (vacuum, He, N<sub>2</sub>, Ar). Our test unit allowed to simulate real work regimes during synchrotron experiments for 2 and 9 hours.

After samples exposition under the white beam, we observed changes in topography of the irradiated areas of some samples. Surface degradation was corresponded to blisters development. Blisters density and size were investigated by optical microscopy and scanning electron microscopy. Chemical composition of the samples prior and after irradiation was checked by the Auger electron spectroscopy and Rutherford backscattering spectroscopy.

It was shown that character of blister formation strongly depended of the irradiation conditions, such as exposition time, type of gas atmosphere, pressure and thickness of the coatings. Blisters took place only at small irradiated areas, which equaled to the area of the X-Ray beam. The largest impact was induced by the gas atmospheres. The most aggressive environment appeared to be helium atmosphere. Density of the blisters after white beam test in 1.1 Bar of He atmosphere exceeded 500 blisters per mm<sup>2</sup>, while it was less than 60 blisters per mm<sup>2</sup> for white beam test in vacuum.

Mechanism of blisters formation will be discussed as well as the ways for weakening of blisters development by changing the choice of precursor. Perspectives of using thin film protective coatings for beryllium X-Ray optical elements are up to experiment conditions.

## **Tatiana Zakharchenko**

[t.zakharchenko@fmlab.ru](mailto:t.zakharchenko@fmlab.ru)

Department of Material Science, Lomonosov Moscow State University

**PhD student**

Russia, 119991, Moscow, GSP-1, 1-73 Leninskiye Gory, Laboratory  
Building B

**Research interests:** Lithium-air battery, Small Angle Neutron  
Scattering



### **Small Angle Neutron Scattering Study of the Mechanisms Limiting Li-air Battery Capacity**

Li-air batteries are often considered to be the next generation battery technology, as theoretical predictions promise outstandingly high energy density around 1000 Wh/kg [1]. Such expectations are based on the low weight of active materials: metallic lithium (at the anode) and oxygen (at the cathode). To facilitate charge transfer and to provide space for insoluble reaction product ( $\text{Li}_2\text{O}_2$ ) a conductive porous matrix most commonly made of carbon black is used as a cathode in Li- $\text{O}_2$  cell.

Optimizing of cathode morphology (pore size distribution, specific surface area) for the best cell performance is subject of many experimental [2] and theoretical [3] works, however it's lack of the data about cathode pores filling by  $\text{Li}_2\text{O}_2$  during discharge, because most frequently technique for studying it - SEM [2] says nothing about the distribution of the peroxide in the depth of the electrode. Here we first propose small-angle neutron scattering (SANS) study of carbon electrodes of Li-air battery cell. By this method 1-100 nm diameter pores can be investigated that, according to  $\text{N}_2$  absorption data, contribute most to the specific surface area. Additionally, in contrast to standard methods of pores size distribution evaluation, by tuning the isotopic composition of electrolyte SANS allow us to study samples wetted by variety of electrolytes and so get information about surface area that available for electrolyte and consequently electrochemical active.

Carbon paper was used as an electrode material with controlled porosity. It was found that pores smaller than 10 nm diameter aren't wetted by DMSO-based electrolyte so they don't take part in oxygen reduction reaction. After filling app. 50% percent of 10 - 100 nm diameter pores by discharge product further discharge blocks regardless of the discharge current rate. Also formation of periodical structures with correlation length of about 3.5 nm was found that could be attributed to  $\text{Li}_2\text{O}_2$  spherulites previously observed by SEM [4].

Based on these data we proposed model of cathode pore filling during battery discharge that can be used for further optimizing cathode structure.

[1] J. Christensen, et al., J. Electrochem. Soc R1 (2012)

[2] S. R. Younesi, et al., J. Power Sources 9835–9838 (2011) 196

[3] A. V. Sergeev, et al., J. Power Sources. 707–712 (2015) 279

[4] T.K. Zakharchenko, et al. Beilstein J. Nanotechnol. 758 (2013) 4

## Peng Zhang

[Peng.zhang@leibniz-inm.de](mailto:peng.zhang@leibniz-inm.de)

Leibniz Institute for New Materials

Postdoc

Campus D2 2 Saarbrücken, Germany

**Research interests:** Supramolecular structure; Polymer nanocomposites; X-ray scattering



### In situ SAXS Study of Formation of Crystalline Supramolecular Structures in a Fluoroalkyl Ionic Liquid

Ionic liquid crystals combine the properties of ionic liquids and liquid crystals and are interesting model systems for the study of structure-property relationships in soft matter. Coulomb interactions that stabilize the mesophase can lead to uncommon crystalline structures.[1] We studied in situ the supramolecular structure formation in a fluoroalkyl ionic liquid,  $[\text{P}(\text{Bu})_3(\text{CH}_2)_2(\text{CF}_2)_{10}\text{F}][\text{N}(\text{CN})_2]$ , with small angle X-ray scattering (SAXS). Figure 1a shows a typical 2D SAXS pattern that indicates a crystalline structure in the fluoroalkyl ionic liquid at 20 °C. The crystal melts upon heating while the mesophase structure remains stable until at least 120 °C (Figure 1b). The non-fluorinated analogous alkyl ionic liquid,  $[\text{P}(\text{Bu})_3(\text{CH}_2)_{11}\text{CH}_3][\text{N}(\text{CN})_2]$ , does not show any crystalline feature at temperatures above -20 °C (Figure 1c).

The fluoroalkyl ionic liquid shows a lamellar structure with a periodicity that is larger than the molecular size (arrows in Figure 1b). The lamellae form through the combined actions of Coulomb and van der Waals forces. The lamellar structure stabilizes a crystalline structure, because it allows the interdigitation of the fluorinated segments.[2] This stabilizes a highly ordered arrangement that does not occur in the non-fluorinated liquids. We use this model system to study the coupling between crystallinity and supramolecular structure formation and explore the relevant formation mechanism via *in situ* SAXS.

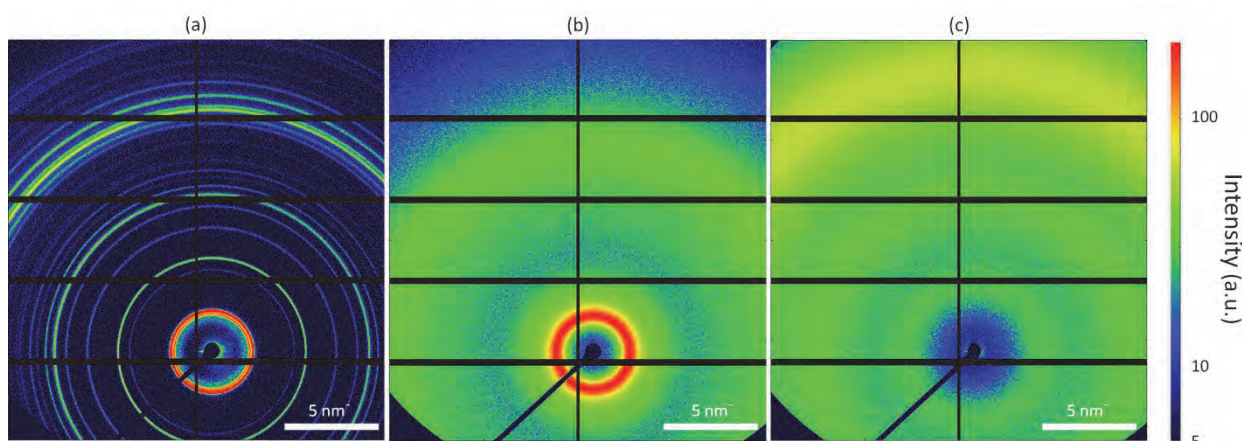


Figure 1 Typical 2D SAXS data showing the crystalline (at 20 °C) (a) and amorphous (at 100 °C) (b) structures of a fluoroalkyl ionic liquid  $[\text{P}(\text{Bu})_3(\text{CH}_2)_2(\text{CF}_2)_{10}\text{F}][\text{N}(\text{CN})_2]$ . Panel (c) showing the typical structure (at 20 °C) of the analogous non-fluorinated alkyl ionic liquid  $[\text{P}(\text{Bu})_3(\text{CH}_2)_{11}\text{CH}_3][\text{N}(\text{CN})_2]$ .

[1] K. Binnemans, Chem. Rev. **2005**, 105, 4148.

[2] T. P. Russell, J. F. Rabolt, R. J. Twieg, R. L. Siemens, and B. L. Farmer, Macromolecules **1986**, 19, 1135

Passed for printing: 2016  
Digital printing.  
Circulation: 150 copies. Order 50

Printed in NRC «Kurchatov Institute»  
123182, Moscow, pl. Akademika Kurchatova, 1